Optica Applicata, Vol. XXIX, No. 1–2, 1999

Multicore single-mode soft-glass optical fibers

RYSZARD ROMANIUK

Warsaw University of Technology, 00–665 Warszawa, Poland.

JAN DOROSZ

Biaglass Co. and Technical University of Białystok, 15–139 Białystok, Poland.

The work presents recent developments of chosen aspects of optical fiber technology at the Research Production Department of Fiber Optics (FOD) at Biaglass Co. The modified multicrucible (MMC) technology of optical fibers, referred shortly to, throughout this work, as the MMC process was used to obtain several kinds of usable optical fibers for sensors and functional components of fiber microoptics. The MMC fibers, which are analyzed in this paper, are triple-core, double-core and twin-core, also quadruple-core ones. These fibers belong to the broader family of multicore optical fibers (MOFs). Such fibers introduce a few of new possibilities to the transmissive or sensory photonic system design: wave and core multiplexing, internal in-fiber interference and multichannel property. These features are subject of research in this work. Some of the unique properties of MOFs seem to have been shown (calculated and measured) for the first time.

1. Introduction

Several cylindrical cores can be distinguished in a MOF [1]. The cores may be embedded in a homogeneous common cladding, in the simplest case of fiber construction. The core can have complex structure (mechanical, refractive, attenuating, *etc.*) in a complex multicore fiber. Guiding parameters of MOF like: number of cores, core distribution, modal characteristics and others are defined by the distribution of refractive index in the fiber cross-section $n(x, y)$ [2]. The simplest out of these are step index multicore optical fibers, which are here the main subject of investigations. The MOFs can also be manufactured as gradient ones. The main parameters for step index multicore optical fibers are refractive indices of cores and cladding, core diameters, core separation, core topology and dispersive properties of fiber material. It is just these parameters that the work focuses on.

Figure 1 presents the simplest solutions to MOF: twin core and double core optical fibers. More cores in a common cladding offer many possibilities of their mutual distribution against the fiber axis, thus, obtaining profoundly different fiber properties. A number of new multicore fiber configurations have been analyzed for the first time. Theoretical considerations have been supported by measurements of chosen samples of multicore optical fibers. The fiber samples were manufactured by original method devised by the authors. The eigenvalue equations have been solved

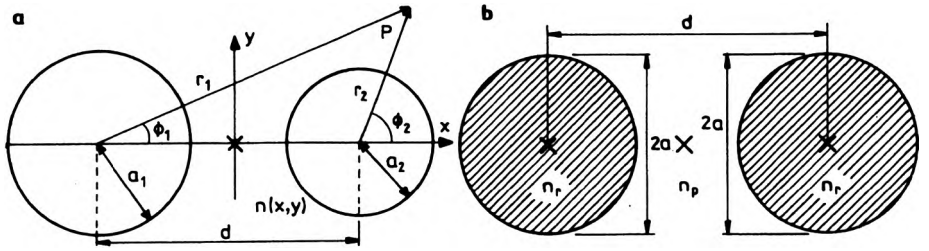

Fig. 1. Circular, double-core (cores non-identical) — **a**, and twin-core (cores identical) — **b**, optical fiber geometry. r_1, r_2 — distance to analyzed point of electromagnetic field P, a_1, a_2, a_3 — core diameters, d — distance between core centers, Φ_1, Φ_2 — angles to analyzed point P from core axes, X fiber center, $n(x, y)$ — refractive index profile of the fiber, n_r — refractive index of core (in the case of step index profile), n_p — refractive index of cladding (in the case of step index profile), cladding boundary not shown in the picture.

for a number of multicore optical fibers. Thus, we were able to present some of their guiding, dispersion, coupling and birefringence properties. Some of these parameters for multicore optical fibers (with more than two cores) differ profoundly from these known for single-core optical fibers [2] and for those known for twin-core optical fibers [3].

The analysis of twin and double core optical fibers is quite well known [2]–[4]. This theory is employed here only as a kind of general background and is not used directly. We present our approach for several reasons. We make our own calculations to support the technology of these kinds of fibers at Biaglass Co. The calculations are focused on particular parameters of manufactured fibers and materials applied. A very important additional reason is that these fibers are available in samples from FOD Laboratory of Biaglass Co. for all interested research groups. Some of the particular guiding properties of these fibers are presented below. The guiding properties of MMC twin and double core optical fibers are a kind of reference platform for much more complex multicore optical fiber structures also manufactured at FOD of Biaglass Co.

The properties of general solutions of MOFs are not yet known so well as for twin-core optical fiber. Thus, this work mainly focuses on analysis of single-mode triple-core and quadruple-core optical fibers. It is needless to say that the availability of multicore optical fibers (including twin, double and multi-fold) of practically arbitrary design is scarce in the world and the local availability and, thus, possibility to make individual research on them is a great challenge and cannot be overestimated. This is the result of a long research effort and considerable investments in these fields at Biaglass Co. and cooperating institutions.

We also present, for the first time in this work, a totally new approach to fiber measurement and analysis. A world wide web (www) based programming environment was built to enable any net user to measure and analyze their fibers. The site is accessible through a www browser under the Internet address (nms.ipe.pw.edu.pl) [5]. This fiber optics site will be developed and will gather all fiber-optic measurement data, for reference and comparison purposes, from various cooperating photonics research laboratories.

The work focuses mainly on the results of our own calculations of some properties of multicore optical fibers manufactured by us. Most of them are fibers of the same cores and thus are called: twin-, triple-, quadruple-, quintaple-core, *etc.*, in opposition to double-, three-, four-core, *etc.* The latter mean fibers with various cores in a common cladding. Some of the MOFs have been measured for direct immediate comparison with theoretical calculations. But the main group of experimental data on these fibers will be published soon in a separate paper. The measured fibers served as an example of the immense possibilities of the MMC technology developed by us. The photographs of these fibers were presented as insets next to the theoretical models of investigated MOFs of particular topology of cores in the cladding. There is probably (or at least we have not found it in the available references) no other single laboratory, active in optical fiber technology, which would offer such a broad spectrum of tailored single-mode and multi-mode soft glass optical fibers.

The fibers are manufactured from soft glasses, thus their spectral, dispersion, mechanical, elastooptical, and other parameters are quite different from some of the fibers well described in the literature [2]. Very light oxides give fibers of low losses in the short wavelength region, while application of very heavy oxides of high purity in the MMC process results in fibers transparent even up to 2 μm. Thus, the spectral region of concern for our fibers spans from near UV up to over 2.5 μm.

2. Calculations of core coupling in multiple-core optical fibers

While analyzing the core coupling in a MOF a few standard initial values have to be defined and initial conditions assumed [3]. The initial conditions are that the cores separation is comparable to the core radius, fiber is weakly guiding, refractive index has step character, geometry is perfectly circular. In such a case, the fundamental guided mode of an excited core overlaps the region of the adjacent core. Optical power cross-talk, of periodic character, is a result of this process. The coupling coefficients between two adjacent cores are [4]:

$$C_{ij} = C_0 \int_{A_j} n_j^2 \Psi_i^{\text{clad}} \Psi_j^{\text{core}} \, dA, \quad i \neq j, \quad i, j = 1, 2$$

where $C_0 = \dfrac{k\sqrt{\varepsilon_0}}{4\sqrt{\mu_0 N_i N_j}}$, Ψ – electromagnetic fields, $k = 2\pi/\lambda$ – free-space wave number, $N = (\pi a^2 n_{\text{core}}/2)\sqrt{\dfrac{\varepsilon_0}{\mu_0}}\dfrac{V^2}{U^2}\dfrac{K_1^2(W)}{K_0^2(W)}$ – standard field normalization to orthonormal modes, A_j – cross-section of the j-th core, Ψ^{clad}, Ψ^{core} – respective fields in cores and cladding, $U = a\sqrt{k^2 n_{\text{core}}^2 - \beta^2}$ – core modal parameter, which is an argument of the core wave function, $W = a\sqrt{\beta^2 - k^2 n_{\text{clad}}^2}$ – cladding modal parameter, which is an argument of cladding wave function, $V^2 = k^2 a^2 (n_{\text{core}}^2 - n_{\text{clad}}^2) = U^2 + W^2$ – normalized frequency. Orthonormal field parameter N is originally proportional to an integral from scalar product of guided fields

[2] and the expression in the simplified form as presented above is possible when we assume that the guide operates in a limited range of normalized frequency V, around single-mode condition. The core and cladding wave arguments U and W are a linear function of V of the following form: $W = 1.1428 - 0.0996$ for $1.5 \leqslant V \leqslant 2.5$. The accuracy of this simplification is better than 0.2% [2].

Assuming further simplifications [6], [7] which are obvious, such as omission of self-coupling effects, using known expansion of K functions and known substitutes for integrals of Bessel functions, one can obtain the coupling coefficients in the analytical form. For all M cores in the MOF the equation for coupling coefficient has to be rewritten to the form including the analogous sum of integrals calculated over $M-1$ cores

$$C_{ij}^{M} = C_{ij} + C_0 \sum_{\substack{\text{core}=1 \\ c \neq i,\, c \neq j}}^{M} \int_{A_c} n_{\text{core}}^2 \Psi_i^{\text{clad}} \Psi_j^{\text{clad}} \, dA.$$

The second factor in the equation is the coupling between the i-th and the j-th cores holding over the adjacent cores between them and is negligible. This is only in the case when the coupling between non-adjacent cores can be omitted, or when a coupling to a single neighbouring core predominates. When this assumption is not fulfilled, the coupling coefficient in a MOF cannot be expressed in a simple form, because the power in each core is a complex superposition of modes from different cores. The phase relations of cross-talk never reach 0 – 1 values for complex MOFs as in the case of an ideal twin-core optical fiber.

The analytical form of coupling coefficient between adjacent cores in a MOF is, in our simplified case,

$$C_{ij} = C_0 \Theta_{ij}$$

where Θ_{ij} is an algebraic relation of functions I, J and K of the form

$$\Theta_{ij} = \frac{a_j K_0(W_i d/a_i)(W_i/a_i) I_1(W_i a_j/a_i) J_0(U_j) + (U_j/a_j) I_0(W_i a_j/a_i) J_1(U_j)}{K_0(W_i) J_0(U_j)(W_i/a_i)^2 + (U_j/a_j)^2}, \qquad i \neq j,$$

(d – distance between coupled pair of cores). Thus, the coupling between nonadjacent cores is a process of in-series couplings between adjacent ones. Usually, a few other parameters are introduced to facilitate the multicore optical fiber analysis:

– Mean coupling coefficient: $C = \sqrt{C_{12} C_{21}}$.

– Various kinds of normalized propagation constants: $\beta^s = (\beta_1 + \beta_2)/2$, $\Delta\beta = \beta_1 - \beta_2$, $\Delta\beta^r = (\beta_1 - \beta_2)/\beta_1$, $\Delta\beta_{AS}^r = (\beta_{AS} - \beta_{SA})/\beta_{AS}$, $V_p^{AS} = \tilde{\omega}/\beta_{AS}$ – phase velocity, $\beta_N = [(\beta^2/k_0^2 - \varepsilon_{\text{clad}})/(\varepsilon_{\text{core}} - \varepsilon_{\text{clad}})]^{1/2}$ with AS – modal notation, which stands for antisymmetric–symmetric, being explained in mode detail later in this work.

– Power transfer efficiency between cores (and normalized power): $P^{te} = (1 + (\Delta\beta/2C)^2)^{-1/2}$.

– Core power contrast: $P_{ij}^c = (P_i - P_j)/(P_i + P_j)|_{z = mZ_b} = -\cos(2mZ_b C_{ij})$, where Z_b – beat length, $m \in c$, z – distance.

AS is mode designation in double-core (or quadruple-core) optical fiber in terms of symmetric–antisymmetric notation. The differential values of propagation constants are a measure of fiber birefringence. The beating length is defined as a direct function of the coupling coefficient: $Z_b = \pi P^{te}/2C$. From the last dependences, it is seen that C and P^{te} behave like additional propagation constants. This is understandable, since the coupled modes can be treated as new modes propagated by the complex waveguide of multicore structure. The symmetrical–antisymmetrical notation of modes in a double-core optical fiber stems from this simple assumption.

3. Measurements of multicore optical fibers

Measurement techniques of multicore optical fibers require adaptation of special coupling methods for excitation of individual cores and for optical power detection from individual cores. A method was adapted with multifiber fused tapers. If the core distribution in the multicore fiber is simple and homogeneous (*i.e.*, linear equidistant, triangular equilateral, square, hexagonal, *etc.*), it is comparatively straightforward to assembly relevant fiber taper composed of single-core fibers. The fibers should usually have nonstandard proportions between core and cladding.

In the case of nonhomogeneous core distribution in a MOF, it is quite complicated to manufacture a relevant taper from individual fibers. Sometimes it is easier to use the same MMC process with lowered speed of fiber pulling to manufacture much thicker fibers and then make tapers out of these "preform"-like fibers.

A photograph of a multiple fiber taper is presented in Fig. 2**a**. The taper was cut (cleaved) at a proper length for diameter and core spacing match with investigated multicore optical fiber. A typical power detection scheme with homodyne reference channel was applied to measure the output from MOF. Figure 2**b** shows a block diagram of our computer based measuring system for assessing the parameters of optical fibers. The system consists of two major parts: computer management and programming environment, photonic measurement system. Both parts are closely integrated with each other.

One of the most important parts of photonic measurement system is precision V-groove coupler with which it is possible to connect multicore taper with multicore fiber. The V-groove coupler enables tilting of one part of coupled fiber to adjust it to the taper. Also some insight to the coupling is enabled through a microscope view. This insight enables some visual evaluation of coupling quality.

The software of the system consists of four layers presented in Fig. 2. The code is written in LabWindows. Apart from using the native measurement and analysis

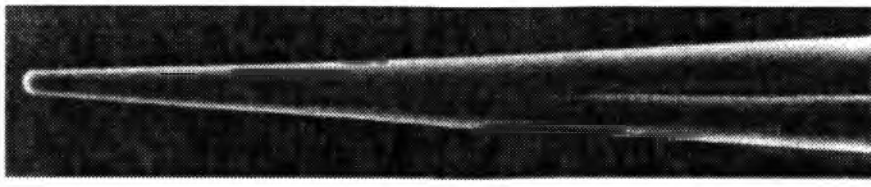

Fig. 2a

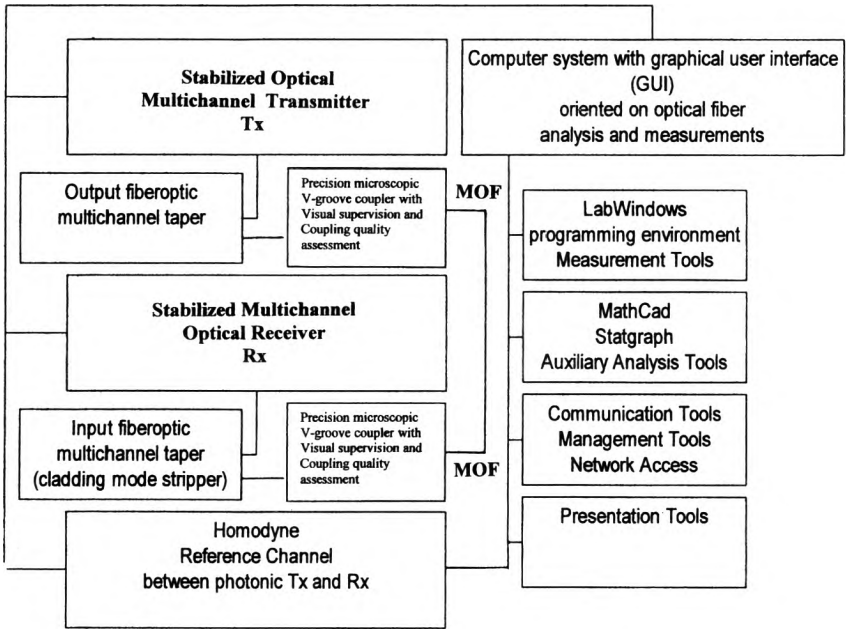

Fig. 2b

Fig. 2. Photonic measurement and analysis system of multiple core optical fiber parameters: **a** – multiple optical fiber single-mode taper for coupling with measured multicore optical fibers (manufactured at FOD of GWB), **b** – block diagram of computer based optical fiber measurement and analysis system including optical power detection scheme applied for measurements of multicore optical fibers.

tools other external tools are used as well, *e.g.*, MathCad and Statgraph. Presentation and library access is done through a friendly graphical user interface (GUI). The GUI features also communication and management tools to share part of the system through the web.

4. Calculations and measurements of core coupling in triple-core single-mode optical fiber

There are two basic core configurations in a triple-core optical fiber. The cores can be distributed in the cladding linearly or triangularly [8], [9]. Other configurations are spun ones [10]. To simplify the analysis, we are interested here in single-mode, triple-core, optical fibers with identical cores. The previous assumptions also hold. We have chosen two exemplary technological samples of triple-core optical fibers for measurements. The cores are spaced homogeneously in both optical fiber geometries, with the separation parameter comparable to the core diameter [11], [12].

The beat lengths for both fiber samples were calculated theoretically and the measurements were done for these calculated beat lengths, using the usual fiber cut-back method. The beam of light was coupled in and out to the fiber with the aid of

specially prepared optical fiber taper aligned microscopically with particular core. Fused multiple tapers were manufactured to match the output core geometry, individually for each case.

According to the theoretical analysis sketched in Sect. 2, the inter-core coupling analysis was made numerically and some results were verified experimentally. The phase relations of cross-talk never reach 0−1 values in MOFs with complex coupled cores, as in the case of ideal twin-core optical fibers. For example, in the relatively simple (perfect) model of three linearly arranged cores, with one of the extreme cores excited, the middle core never propagates full power, which is exemplified in Fig. 3a. The measurements were made for a comparatively short length of coiled triple-core optical fiber. The length was approximately between 3 and 5 meters. At this short length coiling was necessary to immediately get rid of the cladding modes and stabilize the measurements. The measurements were done for single-mode region of the presented fiber for normalized frequency slightly above 2 and wavelength around 1.3 μm. The cut-back method was applied to measure the optical power as a function of fiber length. The measurements agreed practically ideally with the calculations, and taking into consideration measuring path losses. Beating length was around 3 mm (linear distribution of cores) and 1.5 mm (triangular distribution of cores) for these particular fibers. The fibers had cut-off frequencies (normalized) for the values V around unity. Some of the fiber samples were measured for much shorter transmission lengths, which was from 10 cm to one meter. Then the cladding mode stripper was used.

The power is coupled fully to the very opposite core, with the intermediate core serving as a relay. The relay couples the power back and forth between both extreme

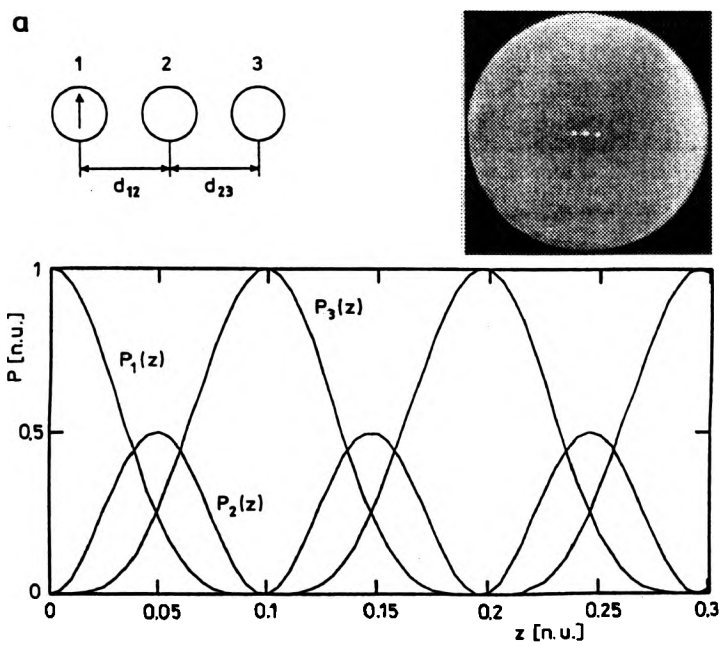

Fig. 3a

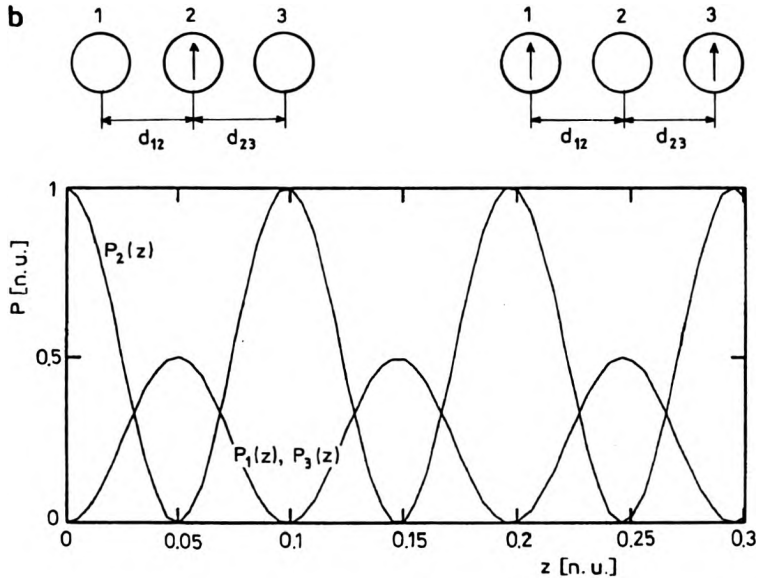

Fig. 3b

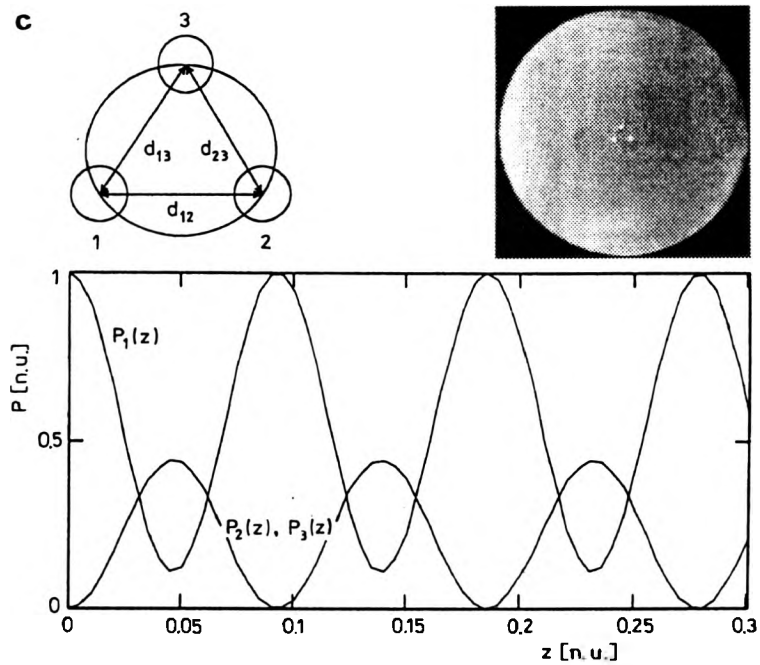

Fig. 3c

Fig. 3. Calculated and measured (they are nearly identical) optical power transfer in a nearly identical, loss-less, identical triple-core, single-mode fiber $P_1(z)$, $P_2(z)$, $P_2(z)$ for two basic geometries of core distribution in the cladding – linear (**a**, **b**) and triangular (**c**). Insets present core excitations and real measured single-mode MMC fibers and details of core geometry. Fiber data: linearly distributed cores: $\varnothing = 120$ μm, $a = 3$ μm, $\Delta = 0.4\%$, $d_{12} = d_{21} = d = 5$ μm; triangularly distributed cores $\varnothing = 120$ μm,

fibers. When the center core is excited, then it couples the power to both adjacent cores (Fig. 3**b**). When the coupling is identical, an outcome is a 3 dB-power divider. When both extreme cores are excited the power sums up in the center core and then couples back evenly to the extreme cores. Extreme cores are not coupled directly but with the aid of the center core, which is a kind of a coupling relay [13]. The situation is the same as in Fig. 3**b**.

When the three cores are arranged in the fiber in perfect circular geometry (the cores are building the equilateral triangle), all of them are coupled identically. Excitation of one core causes identical coupling to two remaining cores evenly like in the case of center core in the linear configuration. But the difference is that the coupled cores (extreme cores in linear configuration case) are now coupled together, unlike in the linear core distribution case. As a result, two bi-directional coupling processes are going on at a time, and the optical power never reaches zero in the excited core, while the remaining two coupled cores are excited identically and in phase. This situation of coupling geometry is also presented in Fig. 3**b**.

The coupling characteristics in triple-core linearly distributed equidistant optical fiber are symmetric due to the symmetricity in core topology. Either non-equidistant triple-core or three-core single-mode can have much more nonsymmetrical coupling characteristics. Changing the distances d_{ij} (as in Fig. 3**a**), one can shift respectively the power coupling curves along the z-axis relatively to the original power excitation curve. One of the boundary cases is when the power in the third core (opposite extreme core) changes in phase with the power in excited extreme core. We may talk of coupling resonance in this case. Such a state has several interesting properties like increased power transfer efficiency and indicates the presence of multiple coupling resonances in multi-core optical fibers. For example, it may be predicted from this simple example that the four-core optical fibers may have two different coupling resonances. These effects are subject of measurements in our laboratory with the usage of MMC multicore optical fibers.

Summing up the core coupling and core spectral properties of triple-core fiber one can say that the fiber possesses in-built "optical relay" properties. It behaves slightly like an electrical relay. The central core, in case of extreme core excitation, acts like optical separating channel. One can assume certain degree of optical nonreciprocity of this channel and an optical insulator is obtained from such a device as a result. This

(Fig. 3, continued) $a = 3$ μm, $\Delta = 0.4\%$, $d_{12} = d_{13} = d_{23} = d = 8$ μm. Optical power and distance expressed in relative normalized units (where: $\varnothing$ – fiber diameter, a – core radius, d_{ij} – intercore distances between i-th and j-th cores, Δ – relative refractive index difference between core and cladding, $P = P_x/P_{max}$ – relative optical power, P_x – branched power, P_{max} – maximum value of optical power. Measurements made for $\lambda \approx 1.3$ μm. Cut-off wavelength was for $V \approx 1$. The distance axis can here be expressed in cm, which indicates exceptional high quality of the fiber technology, and resulting small fiber embedded perturbations. The optical power and beat length values are normalized here only for the purpose of data generalization. These characteristics are nearly the same for all fibers of this family with similar technological and construction data.

condition is fulfilled when $C_{12} \gg C_{32}$, which can be obtained technologically in such a fiber. The third core acts as a nonreciprocal optical power drain.

For complete symmetrical triple-core fiber it behaves like a perfect optical signal summator or signal divider by two (which is equivalent here to subtraction of half of the signal value).

5. Double-core single-mode optical fibers

The fundamental HE_{11}^{x} mode will pass from one core to the other, if the total phase shift $\Delta\Phi$ satisfies the following condition: $\Delta\Phi = (2m+1)\pi$, where m is a natural number. For symmetric–antisymmetric modes notation, being denoted in references [2]–[4], [14] as SA modes, it is equivalent to

$$\Delta\Phi = \omega \int_{-1}^{1} [(V_p^{AS_1})^{-1} - (V_p^{AA_1})^{-1}] ds$$

where: V_p^{AS} is the phase velocity of the given A–S mode. The total energy transfer condition is

$$k_0 \sqrt{\varepsilon_{core}} \int_{-1}^{1} [(1-\Delta(1-\beta_N^{AS_1}))^{1/2} - (1-\Delta(1-\beta_N^{AA_1}))^{1/2}] ds = (2n+1)\pi.$$

For small values of Δ, the expression under the integral is simplified to $\Delta\beta_N^{XX} = \beta_N^{AS_1} - \beta_N^{AA_1}$. Let us assume that one of the cores is excited with HE_{11}^{x}, which is equivalent to the following sum of AS modes: $AS_1 + AA_1$ [3]. At the output we should obtain again HE_{11}^{x} out of the second core, which is equivalent to the following combination of AS modes: $AS_1 - AA_1$.

Let us now see how the fiber material influences the coupling process. We are interested in this influence due to technological reasons for the multicore optical fibers manufactured at FOD of Biaglass Co. When the cores are not identical and initially not coupled strongly, the propagation constants of fundamental HE_{11}^{x} modes in each core are different, β_1 and β_2. Generally, the power transfer directly between the fundamental modes is not easy, as the modes do not match in phase. From the double-core fiber material and waveguide dispersion point of view there is, however, one point on the dispersion characteristic of the fiber, where $\Delta\beta = 0$, for a particular value of $\lambda = \lambda_0^{disp}$. Figure 4 presents calculated dispersion curves of $\Delta\beta^2(\lambda)$ for several samples of double-core single-mode optical fibers (DCOF). The calculations were made by solving the eigenvalue equation for coupled core fiber, according to the above presented analysis.

The dispersion curves for different fibers intersect at several places. They reach zero value for different wavelengths. The value of λ_0^{disp} for double-core optical fiber is increasing with diminishing difference in core dimensions and with increasing height of step profile. The cross-coupling coefficients C_{12} and C_{21} are not equal in a double-core optical fiber. The coupling can be much stronger in one direction, *i.e.*, it is not symmetrical. Consequently, more power propagates, on the average, in one of

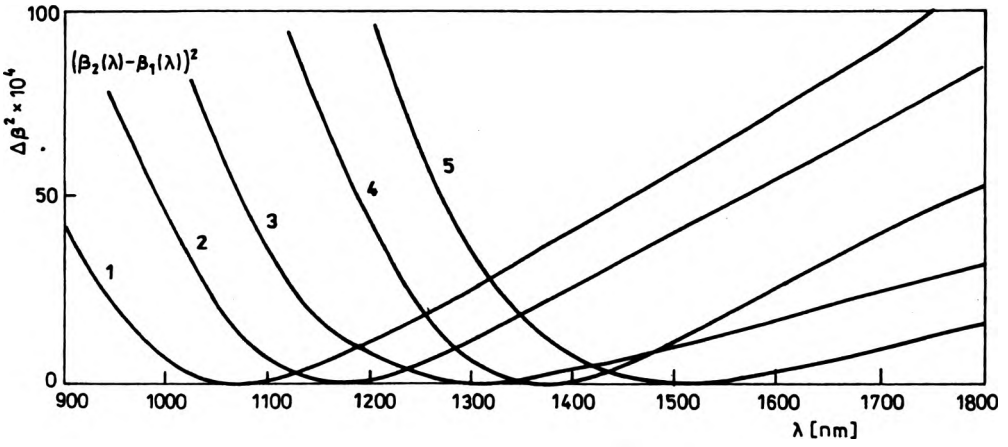

Fig. 4. Calculated dispersion of core birefringence $\Delta\beta^2(\lambda) = \beta_2^2 - \beta_1^2$ (from the eigenvalue equation as shown in the text) in five samples of double-core single-mode optical fibers. Birefringence reaches zero for λ_0^{disp}. This wavelength is a function of fiber geometry and fiber material parameters and shifts to longer wavelengths if cores become more similar. Fiber sample and core data: **1** – core No. 1, $a = 3$ μm, $\Delta = 0.2\%$, core No. 2, $a = 9$ μm, $\Delta = 0.15\%$, **2** – core No. 1, $a = 3$ μm, $\Delta = 0.3\%$, core No. 2, $a = 9$ μm, $\Delta = 0.2\%$, **3** – core No. 1, $a = 3$ μm, $\Delta = 0.4\%$, core No. 2, $a = 9$ μm, $\Delta = 0.2\%$, **4** – core No. 1, $a = 3$ μm, $\Delta = 0.4\%$, core No. 2, $a = 7.5$ μm, $\Delta = 0.2\%$, **5** – core No. 1, $a = 3$ μm, $\Delta = 0.4\%$, core No. 2, $a = 6.5$ μm, $\Delta = 0.2\%$; $d = 10$ μm – for all cases (Δ – relative difference of refractive indices, a – core radius, β_1 β_2 – propagation constants of the first and second core in the common cladding of a double core fiber).

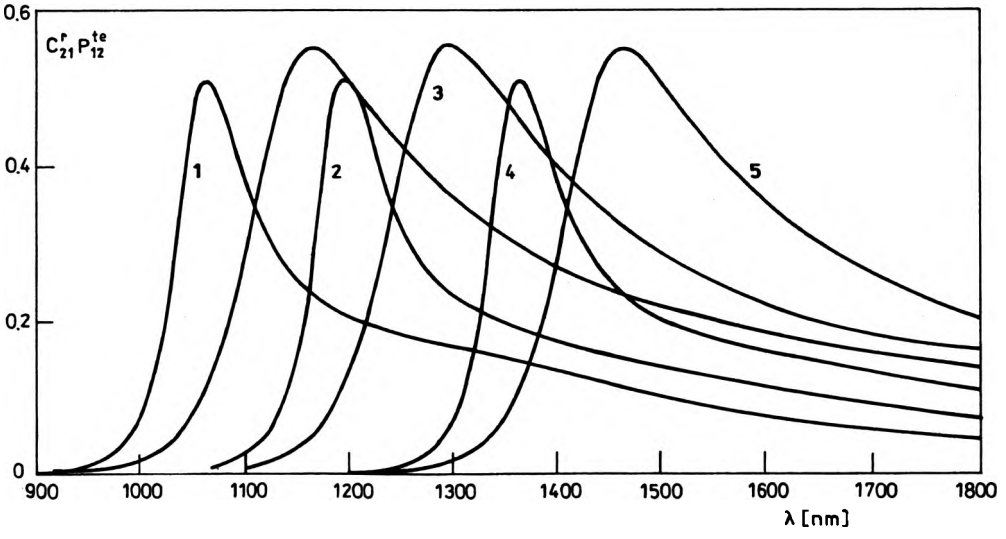

Fig. 5. Calculated dispersion characteristics of effective power transfer efficiency in double-core optical fibers. Fiber samples data the same as in Fig. 4. P_{12}^{te} – power transfer efficiency between cores 1 and 2, C_{21}^r – relative value of coupling coefficient between cores 2 and 1.

the cores. The measure of coupling symmetricity and power transfer efficiency (or de-tuning from λ_0^{disp}) is a coefficient of relative cross-coupling $C_{ij}^r = C_{ij}/C_{ji}$. The plots of the functions $C_{21}^r(\lambda)P_{12}^{te}(\lambda)$, corresponding with curves in Fig. 4, are presented in Fig. 5.

The power coupling efficiency does not exceed 60% in the investigated cases. The coupling efficiency could not be greater for this double-core fiber geometry. Several guided wave processes influence the shape of the coupling efficiency curves. The coupling coefficients increase with wavelength for $\lambda < \lambda_0^{disp}$. For greater inter-core spacings, the coupling generally decreases and is less sensitive to the difference of propagation constants in both cores. The relative cross-coupling coefficient $C_{ij}^r = C_{ij}/C_{ji}$ at the wavelength λ_0^{disp} depends only on the difference in refractive profile heights of both cores.

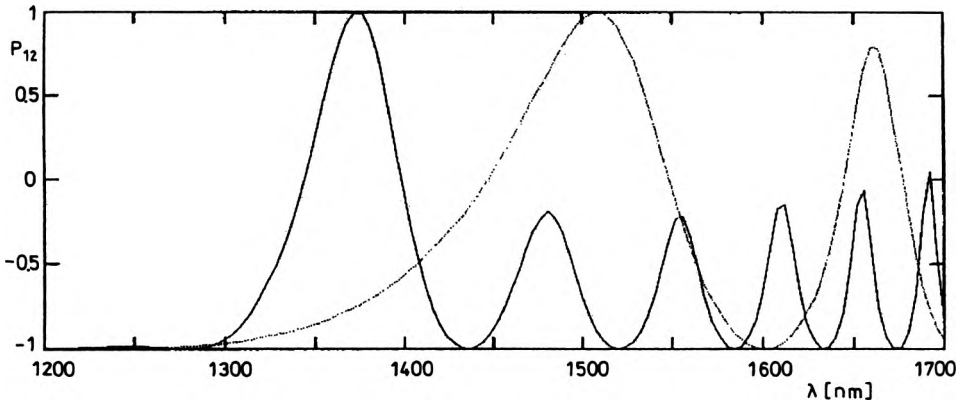

Fig. 6. Calculated dispersion of core contrast in double-core optical fibers. Fiber samples data as in Fig. 4. Here the data are for samples 4 (solid line) and 5 (dotted line). Fiber length is equal exactly to the beat length defined for the wavelength corresponding to the maximum of power transfer.

The power coupling optimization in double-core optical fiber includes such parameters as: core spacing, core refractive profile heights, core diameters and absolute differences of core diameters and profile heights. When one sets the length of the fiber equal to the beat length (for wavelength of maximum power transfer), then the measured output is proportional to the core contrast P_{12}^c. Dispersion of core contrast for some of the investigated fiber samples is presented in Fig. 6.

The spectral coupling characteristics can be narrowed by increasing the core separation parameter. This causes, however, a considerable increase in the needed length of the fiber for Z_b. Figure 7 presents the spectral characteristic of optical power output from the second (larger) core of double-core optical fiber, sample No. 4. This is a typical characteristic of a band-pass filter. Some of these features of the double-core optical fiber can be potentially used in WDM systems. The separation between adjacent bands in an unoptimised optical fiber reaches 40 dB. First results on multicore optical fiber optimization [14] for photonic filtering and

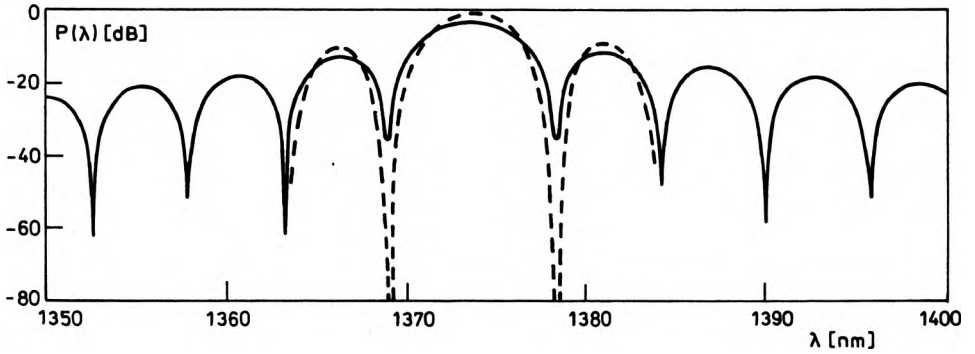

Fig. 7. Calculated spectral characteristic of optical power from the coupled core of the double-core optical fiber, fiber sample No. 4 from Fig. 4. Fiber length $l = mZ_b$ ($m \in N$, and Z_b – beat length). Broken line is a characteristic of a fiber optimized technologically and constructionally for improved band-pass properties [14].

signal processing purposes show that this value can be increased twofold and the bandwidth can be narrowed, as shown in Fig. 7 by broken line. Some of the technological processes for the optimization of multicore optical fiber parameters are subject of patent pending.

6. Influence of glass parameters on transmission properties of twin-core optical fibers

The subject of analysis is here the dependence of the coupling coefficient on twin-core waves and geometrical and optical parameters of the fiber. Thus, we are interested in the fiber manufacturing process design to obtain a MOF fiber of desired coupling properties. The characteristics, which are to be obtained in this section, allow manufacturing of double-core or twin-core MOFs of strictly preset core coupling coefficient. The parameters to be changed during the manufacturing process are the glass choice and some of the technological parameters [15], [16]. The fundamental characteristics of the twin-core optical fiber are presented in Fig. 8 [3].

Figure 1 shows a twin-core fiber of step index profile. The fiber consists of two identical cylindrical cores. The cores are of diameter a and are situated symmetrically against the fiber axis. The distance between the core axes is d. Thus, the core boundaries are at a distance of $d' = d - 2a$ from each other. A normalized intercore distance parameter is introduced $d_N = d'/a = d/a - 2$. The confining case is when $a = d/2$, where $d_N = 0$. The refractive indices involved are n_r for core and n_p for cladding. Weakly guiding conditions are assumed in this analyzed model of MOF fiber. The basic waveguide characteristics of twin-core fiber are presented in Fig. 8.

If the light is coupled to a single core, then the normalized optical power in the second core is $P(z) = \sin^2(Cz)$, where C – core coupling coefficient. The core coupling coefficient is of importance here

$$C = \frac{(2\Delta)^{1/2}}{a}\frac{U^2}{V^3}\frac{K_0(Wd/a)}{K_1^2(W)}, \text{ or beating length } Z_b = \pi/C$$

where: $U = ka(n_r^2 - \beta^2/k^2)^{1/2}$, $W = ka(\beta^2/k^2 - n_p^2)^{1/2}$ – arguments of Bessel function, $V = kan_r(2\Delta)^{1/2}$ – normalized frequency, $\Delta = (n_r^2 - n_p^2)/2n_r^2$ – refractive profile coefficient. We have solved the eigenvalue equation for different sets of technological

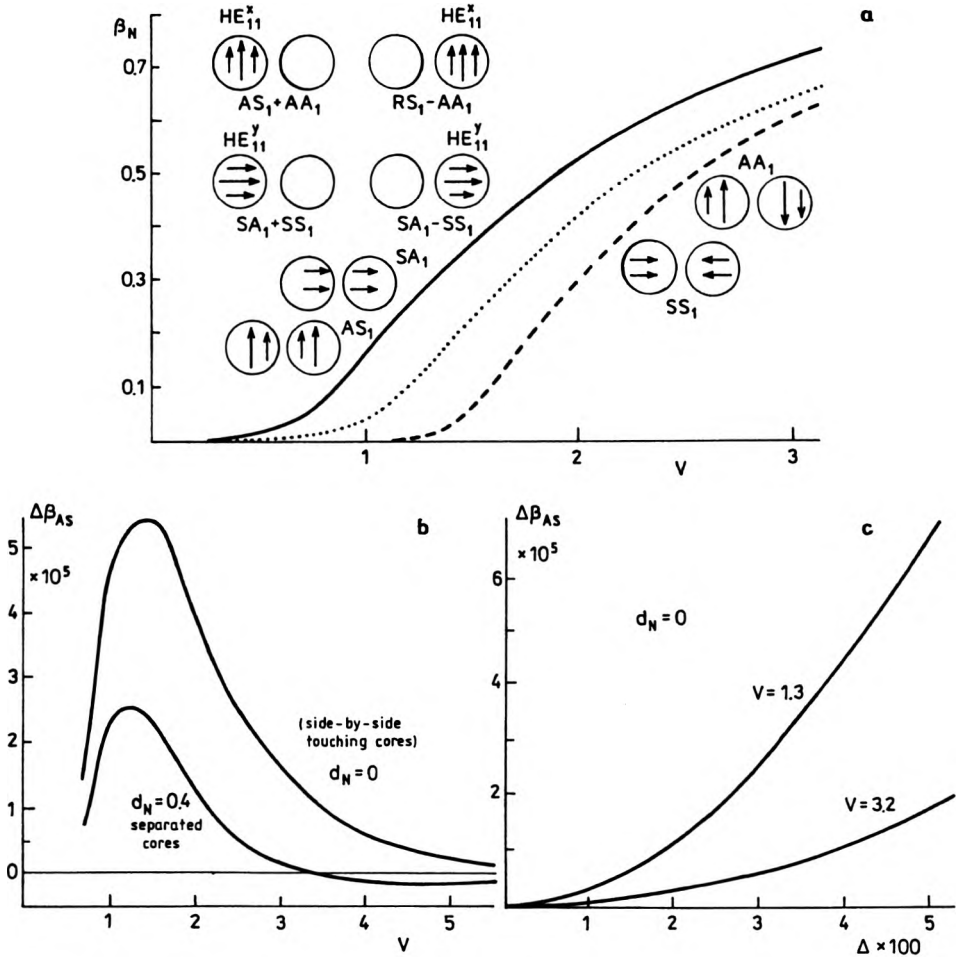

Fig. 8. Basic modal transmission characteristics of single-mode twin-core optical fibers [3]. **a** – fundamental mode dispersion curves $\beta(V)$ for SA_1, AS_1, HE_{11} and SS_1, AA_1 modes., $\Delta = 1.5\%$. The inserts in figure **a** show schematically field distributions in coupled twin (double) cores, or layouts of SA modes. The conventional HE modes in a twin core optical fiber split to SA modes if the cores are close enough. **b** – $\Delta\beta_{AS}(V)$ function for different d_N ($d_N = d/a - 2$), **c** – $\Delta\beta_{AS}(\Delta)$ for $V = 1.3$ (upper) and $V = 3.2$ (lower curve), for touching cores. V – normalized frequency, d – distance between core centers, a – core diameter, d_N – normalized intercore distance parameter ($d_N = 0$ when the cores touch each other or are side-by-side), $\Delta\beta_{AS}$ – differential propagation constant between cores is a measure of intercore birefringence (coupled mode birefringence), $\beta_N = (B_1^2/k_0^2 - n_{clad}^2)/(n_{core_1}^2 - n_{clad}^2)$ – normalized propagation constant for first core.

data out of which two examples are chosen here:

A – $n_r = 1.516$ and $n_p = 1510$, B – $n_r = 1.522$ and $n_p = 1511$.

In comparison with a double-core optical fiber, the twin-core fiber has $C_{21} = C_{12}$ and $\beta_1 = \beta_2$ at $z = Z_b$. The consequence is that the optical power can be transferred with 100% efficiency between cores (at least in an ideal fiber). The coupling efficiency is not dispersive as in a double-core optical fiber. The coupling efficiency does not depend on the wavelength in a twin-core optical fiber. This is a profound difference compared to double-core optical fibers, where all coupling parameters are strong functions of wavelength.

The coupling coefficient in a twin-core optical fiber, and in all other multicore fibers, is a function of wavelength, being thus dispersive. However, all physical non-idealities of the fiber, such as: departure from ideal circular geometry, differences in diameters and refractive profiles, temperature effects, stresses and bends, nonlinear and higher level effects, change the coupling, the beat-length, coupling efficiency and all power transfer phenomena between the cores. The fiber non-idealities (or as seen from the point of view of ideal fiber – second order effects) decide of coupling processes in real-life fibers [16].

The eigenvalue equation was solved for particular material data of investigated fibers. For these particular, single-mode, twin-core fibers, made out of the materials mentioned, the dependence of guided wave beating length was investigated as a function of core separation d and wavelength λ. Figure 9 presents the calculated

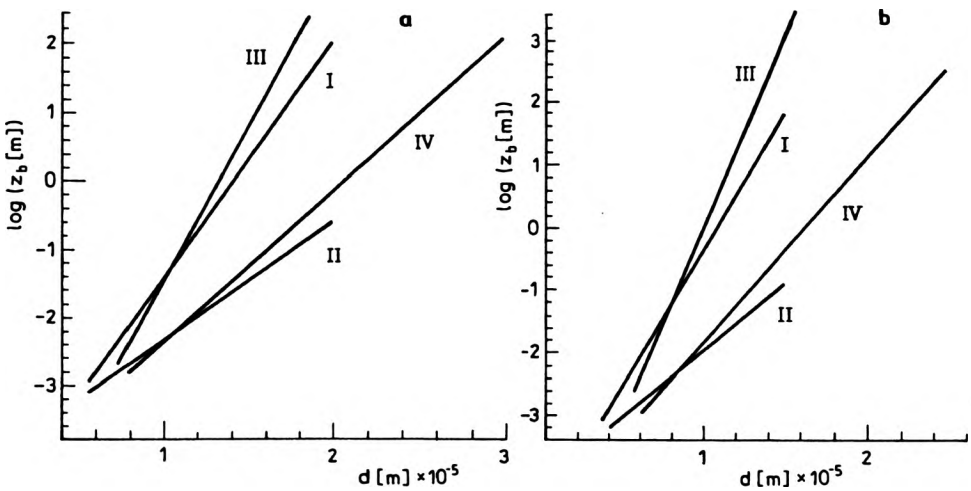

Fig. 9. Calculated material dependent characteristics for samples of twin-core MMC optical fibers. The beat length as a function of core separation parameter $Z_b(d)$ for several samples of twin core MMC fibers of four different core diameters made of two different sets of glasses (a – core radius, d – core separation distance). **a**: A – set of glasses, $n_r = 1.516$, $n_p = 1.510$, fiber core radii and fiber excitation wavelengths are different for the following curves: I – $a = 2.4$ μm, $\lambda = 0.85$ μm; II – $a = 2.4$ μm, $\lambda = 1.3$ μm; III – $a = 3.6$ μm, $\lambda = 0.85$ μm; IV – $a = 3.6$ μm, $\lambda = 1.3$ μm. **b**: B – set of glasses, $n_r = 1.522$, $n_p = 1.511$, fiber core radii and calculated wavelengths for the curves: I – $a = 1.75$ μm, $\lambda = 0.85$ μm; II – $a = 1.75$ μm, $\lambda = 1.3$ μm; III – $a = 2.7$ μm, $\lambda = 0.85$ μm; IV – $a = 2.7$ μm, $\lambda = 1.3$ μm.

value of beat-length Z as a function of d. The function $\log Z_b(d)$ is linear for all combinations of parameters λ and a. The fiber parameters were carefully chosen so as to make them single-mode.

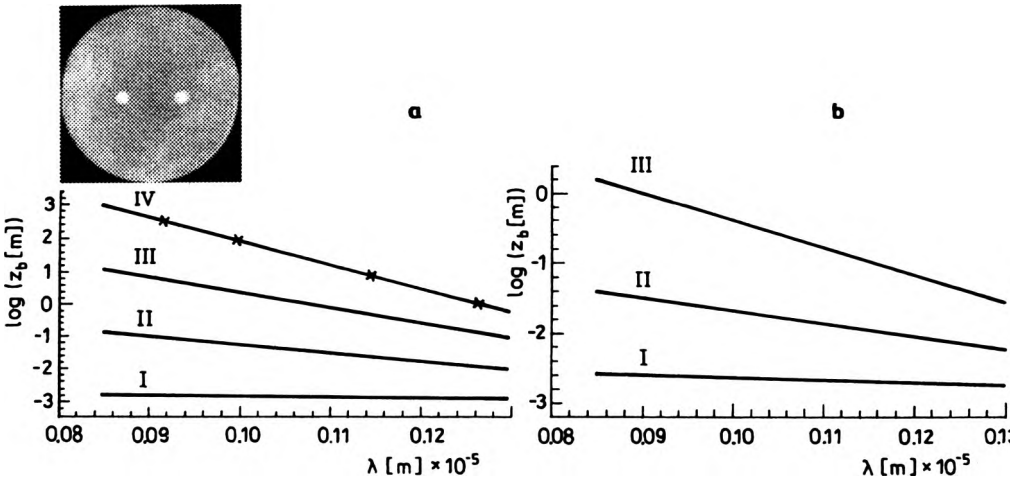

Fig. 10. Calculated material dependent characteristics of twin-core MMC optical fiber. The beat length as a function of wavelength $Z_b(\lambda)$ for MMC twin-core fibers of two different core radii: **a** — 2.4 μm, **b** — 2.0 μm and several different values of core separation parameter and for A set of core-cladding glasses. **a** — $a = 2.4$ μm, I — $d = 5.5$ μm, II — $d = 11$ μm, III — $d = 16.5$ μm, IV — $d = 22$ μm. **b** — $a = 2$ μm, I — $d = 6$ μm, II — $d = 10$ μm, III — $d = 1.5$ μm. The figure shows also comparison between theory and measurements. The crosses on curve IV, (Fig. **a**) indicate measuring points for twin-core optical fiber presented on the photograph. The measurements were done in the same way as presented in Figs. 3 and 4. Fiber end was ground and then polished out with sub-micrometer accuracy. The external diameter of the fiber sample in the photo was ∅ 65 μm and the rest of data as for sample No. 4: $2a = 4.8$ μm, d — 22 μm.

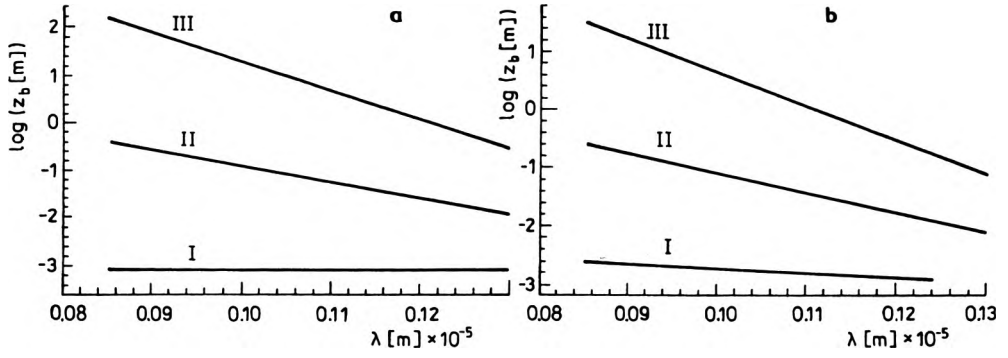

Fig. 11. Calculated material dependent characteristics for manufactured samples of twin-core MMC optical fiber. The beat length as a function of wavelength $Z_b(\lambda)$ for MMC twin-core optical fibers of two different core radii 1.5 μm and 1.75 μm and several different values of core separation parameter and for B set of core-cladding glasses. **a** — $a = 1.75$ μm, I — $d = 6$ μm, II — $d = 10$ μm, III — $d = 15$ μm, **b** — $a = 1.75$ μm, I — $d = 6$ μm, II — $d = 10$ μm, III — $d = 15$ μm.

Figures 10 and 11 present the numerically calculated beat length as a function of wavelength $Z_b(\lambda)$. Comparison of the drawings in these figures shows a strong dependence of beat-length on wavelength. The calculated dependences have important practical meaning, because they allow some technological conditions to be determined for double and twin-core optical fibers of designed coupling between the cores. Figure 12 shows core contrast in a twin-core optical fiber, analogously to the

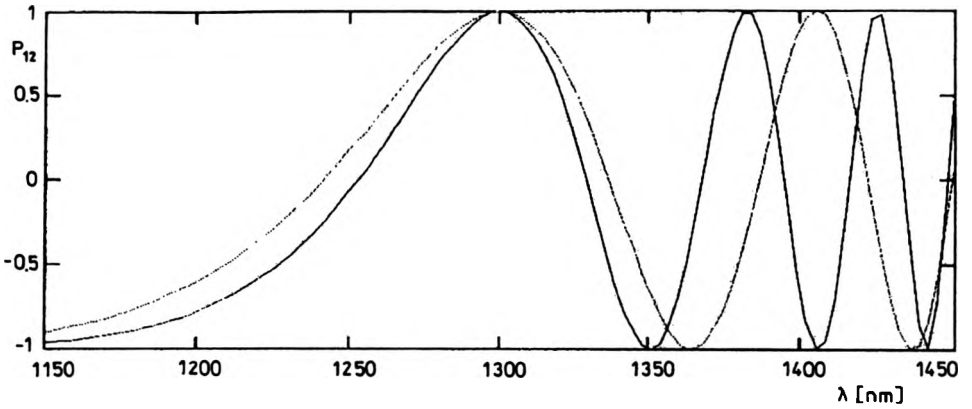

Fig. 12. Calculated dispersion characteristic of core contrast P^c_{12} in two samples of twin-core optical fiber and slightly different core excitation conditions. Sample 1 – core $a = 3$ μm, $\Delta = 0.4\%$, $d = 3$ μm, $V = 2.2$. Sample 2 – core $a = 2$ μm, $\Delta = 0.4\%$, $d = 4$ μm, $V = 1.5$.

core contrast of double-core fiber from Fig. 5. Here, however, the power transfer is non-dispersive and always equals 100%. Similar characteristics were previously calculated for quadruple-core optical fibers [14].

Summing up the twin- and double-core fiber properties, it is seen that they not only exhibit efficient coupling properties but also have strong band-pass characteristics. Recent research [17] indicates that these characteristics can be enhanced or suppressed by fiber bending or fiber design, for example introduction of stress induced agents in an analogous way as in Panda or Bow-tie single-core fibers. Concatenating double-core optical fibers of slightly different parameters leads to narrow band-pass guided wave filters with bandwidth of just a few nanometers and very low losses [17].

7. Quadruple-core optical fibers

We solved the eigenvalue equation [17] for a quadruple-core optical fiber for square, linear and triangular distributions of the cores. Here we will present more data for the square geometry. The coupled modes can be described systematically in terms of symmetric–nonsymmetric notation SA. All standard HE/EH or simplified LP (linearly polarized) [2] modes can be derived from SA modes as spherical or degenerate cases by means of SA mode interferences. Thus the SA notation shows itself as a kind of modal picture generalization in multicore optical fibers of axial (or

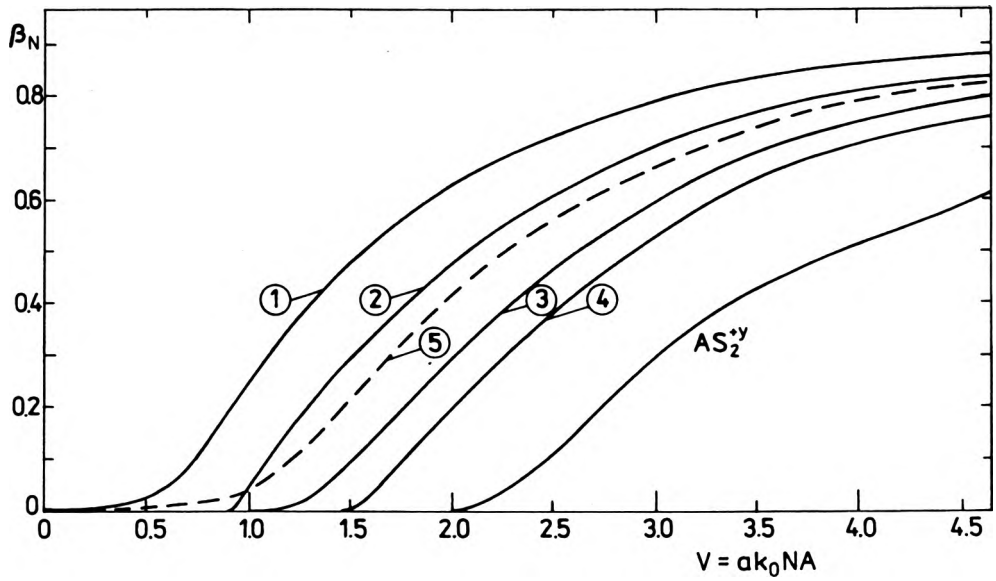

Fig. 13. Normalized propagation constants as a function of normalized frequency (dispersion characteristics) of fundamental modes of single-mode and low-mode quadruple-core optical fiber [16]. Fiber data: $a = 2.5$ μm, $d = 5.5$ μm, n (core) = 1.6, step-index. $\beta_N = (\beta^2/k_0^2 - \varepsilon_5)/(\varepsilon_1 - \varepsilon_5)$, $n_1 = n_2 = n_3 = n_4 > n_5$. 1 – SA^{+x}, SA^{-x}, AS^{+y}, AS^{-y} two-index mode family. 2 – three-index mode family, *e.g.*, SAA^{+x}, ASA^{-y}, *etc.* 3 – $S^{\pm x}$, $S^{\mp x}$, $S^{\pm y}$, $S^{\mp y}$, $A^{\pm x}$, $A^{\mp x}$, $A^{\pm y}$, $A^{\mp y}$, single-index mode family. 4 – $SA^{\pm y}$, $SA^{\mp y}$, $AS^{\pm x}$, $AS^{\mp x}$. 5 – reference curve for HE_{11} mode (SA – symmetric–antisymmetric modes, AS – antisymmetric–symmetric modes, SAA – symmetric–antisymmetric–antisymmetric modes, *etc.*, β – propagation constant, β_N – normalized propagation constant, n ($i = 1, 2, 3, 4$) – refractive indices of four cores, n ($i = 5$) – refractive index of cladding, k_0 – wave number in the free space, ε_i – dielectric permeabilities corresponding to particular regions of multicore optical fiber).

plane) symmetricity. The solution of the equation gives normalized propagation constants for the SA modes in a quadruple core optical fiber [14].

Figure 13 presents calculated values of cut-off frequencies for the lowest orders of SA modes.

The quadruple-core optical fiber of perfectly square distribution of single-mode cores possesses double square symmetry with four symmetry planes shifted by 45°, along the fiber axis, and four symmetry axes in transverse cross-section of fiber, apart from longitudinal axial symmetry. Every additional degree of symmetry of the fiber reflects upon the symmetry and antisymmetry of the transversal vector field pattern of the guided mode. The set of guided modes can be decomposed into orthogonal subsets of symmetric (S) and antisymmetric (A) modes, with respect to available axes or planes of symmetry in the fiber.

A quadruple-core optical fiber with identical cores has four axes of symmetry, and can support theoretically eight subsets of S–A modes: SSSS, AAAA, AASS, SSAA, SAAS, ASSA, ASAS, SASA. The letters S and A describe here the symmetry and antisymmetry of the field H of the guided mode with respect to X and Y axes

(first pair and second pair of letters in the set of four, respectively). The fundamental mode field distributions (field profiles) calculated numerically and showing straightforwardly the idea of S-A modes in quadruple-core optical fiber are presented in Fig. 14. Figures **a**–**d** show fundamental non-coupled modes, while Fig. **e** shows one of the fundamental coupled modes. The initial assumption is that all the cores of the fiber are equally excited at the input face and, after some beating length, specific for this particular coupled mode, the picture is obtained as in Fig. 14**e**. All optical power is propagated only in two cores, with antisymmetric field amplitudes. Assuming a losslees fiber, the field amplitude in these two cores is doubled at the cost of "dead" cores. In the same way other coupling pictures can be obtained including coupled mode families with one "dead" core and three "dead" cores. Besides, the "dead" cores may rotate with fiber length clockwise or anticlockwise. The term "dead" means here no optical power at particular length in the observed core.

The vector H is symmetric (antisymmetric) to both axes for the SSSS (AAAA) modes. The four letter mode names can be abbreviated because the number of symmetrical and antisymmetrical field distributions is exactly known. Thus, we have four major mode families (fundamental modes) in a quadruple-core fundamental-mode optical fiber [14]:

- one-index mode family: S, A,
- two-index mode family: SA, AS,
- three-index mode family: SAA, ASS, SAS, ASA.

There are also possible more complex fundamental mode families resulting from the lowest order mode interference:

- four-index mode family: AS+SA, S or A+(SAA, ASS, SAS, ASA),
- five-index mode family: AS or SA+(SAA, ASS, ASA, SAS),
- six-index mode family is trivial.

The symmetricity of the fiber and, thus, the fields simplifies the set of linear eigenequations describing the system [14]. For S modes, the set consists of four equations for every $m > 0$, and two equations for $m = 0$, each having two solutions (m is the fundamental mode number). Thus, the quadruple-core single-mode optical fiber of square distribution of cores supports the following number of modes (the rest of the mode subsets behave similarly to the S ones):

- two groups of S modes: 2×2 – S^x (called S^{+x} and S^{-x}), S^y (called S^{-y} S^{-y}),
- 2×2 A modes A^x (A^{-x} and A^{-x}), A^y (A^{+y} A^{-y}),
- 2×2 SA modes SA^x (SA^{+x} and SA^{-x}), SA^y (SA^{+y} SA^{-y}),
- 2×2 AS modes AS^x (AS^{+x} and AS^{-x}), S^y (AS^{+y} AS^{-y}),
- 2×8 three-index modes, which could be grouped differently, for example, three-index X modes are: SAA^{+x}, ASS^{+x}, SAS^{+x}, ASA^{+x} and SAA^{-x}, *etc.*

Solving the simplified and properly truncated subsets of eigenequations for each subset of modes separately gives one propagation constant, as presented in Fig. 13, and field profiles of particular modes [14].

The lack of circular symmetry in the fields of a quadruple-core optical fiber of square-core distribution results in the splitting of conventional LP modes into the S-A modes with single-mode subsets faster and slower than LP_{01} (HE_{11}) mode. The

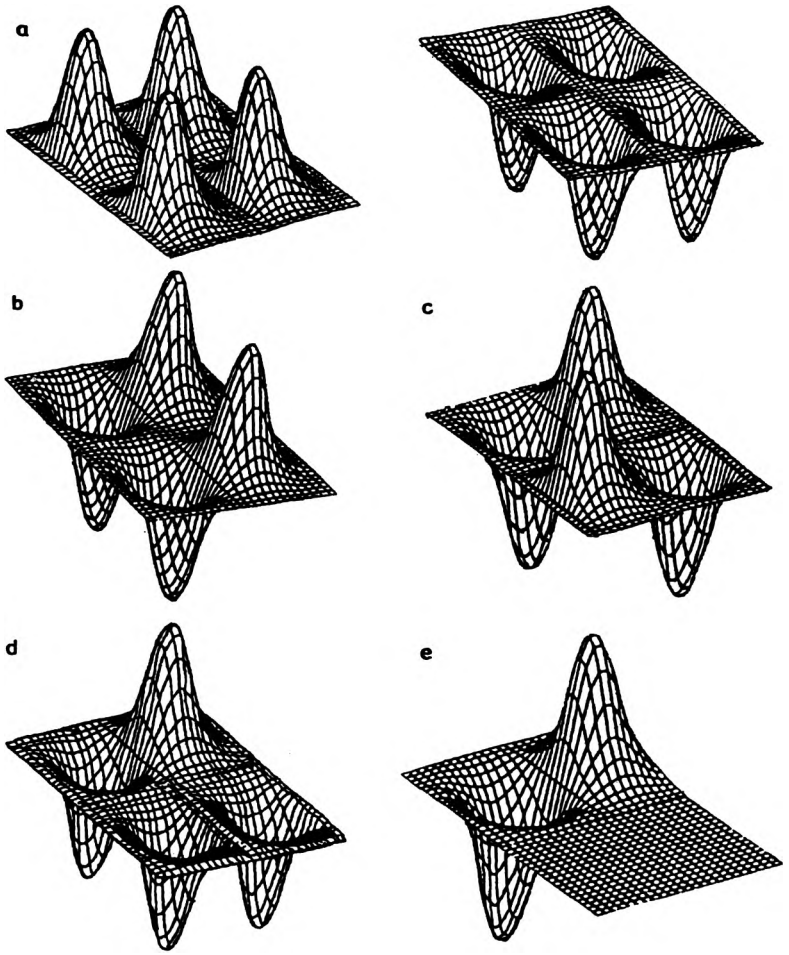

Fig. 14. Computer generated fundamental mode field distributions (field profiles) in a single-mode quadruple-core optical fiber with square distribution of cores. **a** — fundamental symmetric mode S — abbreviated mode name, SSSS — full mode name. **b** — fundamental symmetric—antisymmetric mode, SA, (SSAA). **c** — fundamental antisymmetric A mode, A, (AAAA). **d** — fundamental symmetric SA mode, SAS, (SASA). **e** — coupled antisymmetric SA mode ASA = SAS+ASS, A+SA.

splitting ratio grows with the cores getting nearer. Only the SA_1^x and AS_1^x modes possess no cut-off. The rest of the fundamental modes have nonzero cut-off frequency:

- three index mode family for V around 0.9,
- one index mode family for V around 1.0,
- SA^y, AS^x modes for V around 1.5.

The table presents all SA modes in a quadruple-core optical fiber with square distribution of cores. Figure 15 shows schematic representation of the transversal H field distribution of the SA modes discussed (called core field patterns). The SA

modal field patterns for twin-core optical fiber were added for comparison. One can infer from the calculations and the presented patterns the coupled field patterns with one, two and three "dead" cores. Thus, the SA system of modes describes perfectly the coupling behaviour of multicore optical fibers.

One "dead" core pattern is a combination of the following fundamental modes: S+SAS, S+ASS, S+ASA, S+SAA, S+SAS, S+ASS, A+ASA, A+SAA, SA+SAS, SA+ASS, SA+ASA, SA+SAA, AS+SAS, AS+ASS, AS+ASA, AS+SAA. Two "dead" core pattern is a result of fundamental mode interference between: S+SA, S+AS, A+SA, A+AS, S+A, SA+AS. Three "dead" core pattern (fundamental coupled mode pattern) involved summation of the following fundamental modes: S+SAS, S+ASS, S+SAA.

To have a better insight into the wave and coupling phenomena in quadruple-core optical fiber (and other single-mode multicore optical fibers) we also applied a supplementary, competitive approach of modal power analysis (to the approach of modal fields). A similar inter-core coupling analysis, as for triple double/twin-core optical fibers, presented in the previous sections, was made for quadruple-core ones, with three basic distributions of cores: square, triangular and linear. The results of calculations are gathered in Figs. 16–18, respectively, for linear, square and triangular distributions of cores in the cladding and various geometries of core excitation [15]. These cases exhaust all the simplest and nontrivial solutions. A much more complex analysis is required, however, for all core distribution topologies of interest for potential applications in real-life photonic systems.

Figure 16**a** shows calculated coupling characteristics for quadruple-core optical fiber with linear distribution of cores. The characteristic is for equidistant case, *i.e.*, for equal core separations $d_{12} = d_{23} = d_{34} = d$, and is similar to the linear case of triple-core fiber. Here the 'relaying" property of the fiber is enhanced. The additional core adds more phase shift and latency to the major route of optical power flow. The power accumulates eventually in the fourth core, with the first one excited. Extending this geometry to more cores one is able to notice that the coupling period gets more complicated and recovering of full power in particular core takes much longer time, because of many bidirectional coupling processes present and active at a time.

Core 1 was excited at $z = 0$ in Fig. 16**a**. It is seen from the plot that for relative fiber length $z = 0.125$ virtually all power resides in core 4. Cores 1, 2 and 3 are "dead". For $z = 0.25$ nearly all power is back in core 1, with residual value in the extreme one. Fiber of exactly the same parameters as the one assumed for numerical calculations was manufactured and presented in the inset in Fig. 16**a**. The fiber is now a subject of intense measurements and technological investigations [18] to compare these data with theory and calculations.

Core 2 was excited at $z = 0$ in Fig. 16**b**. The calculated characteristics are also presented for equidistant case. It is interesting to note that the quadruple core coupler with linear distribution of cores and nonsymmetrical excitation has strong nonsymmetrical coupling characteristics. All power is coupled from second to

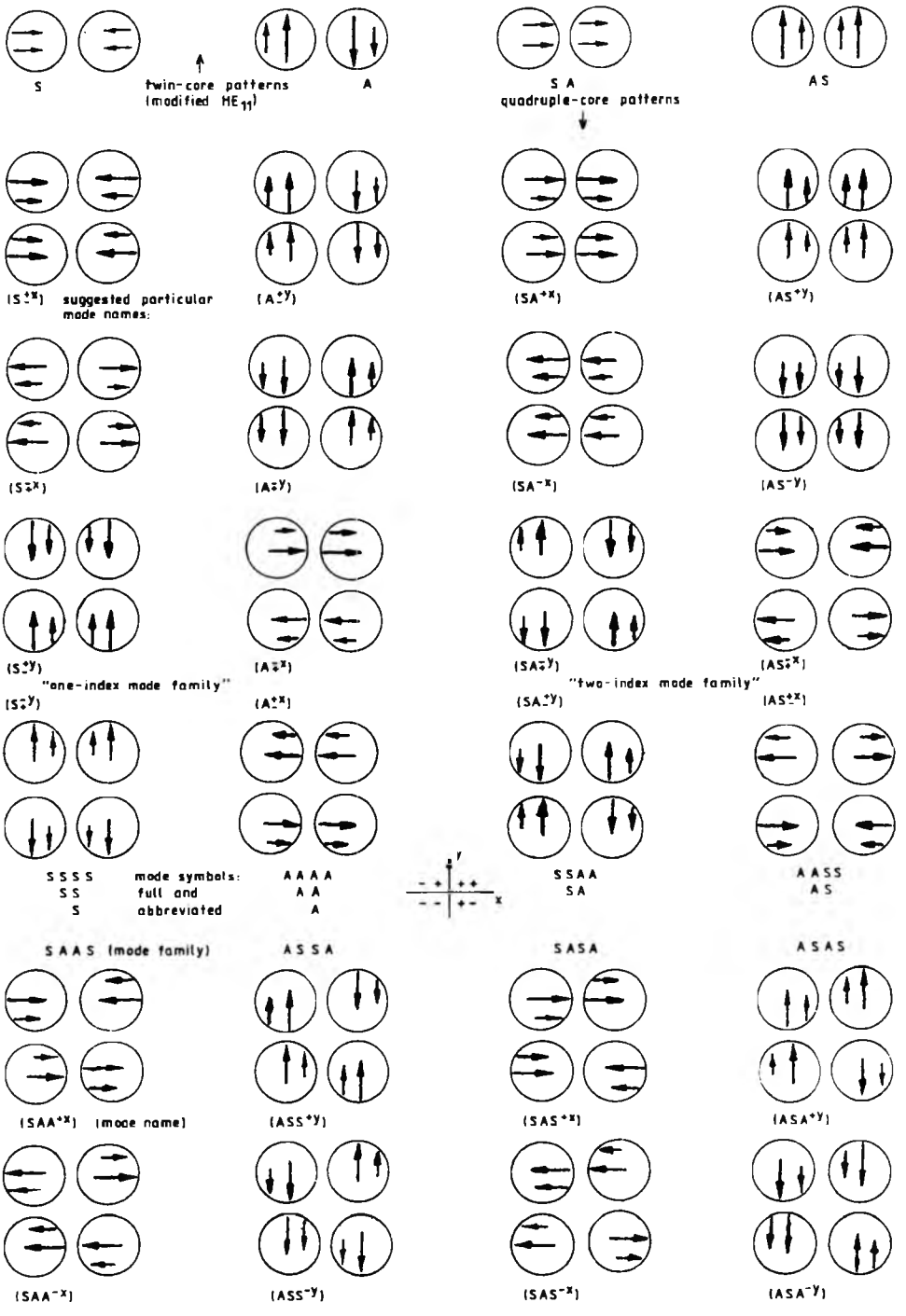

Fig. 15 (to be continued on page 37)

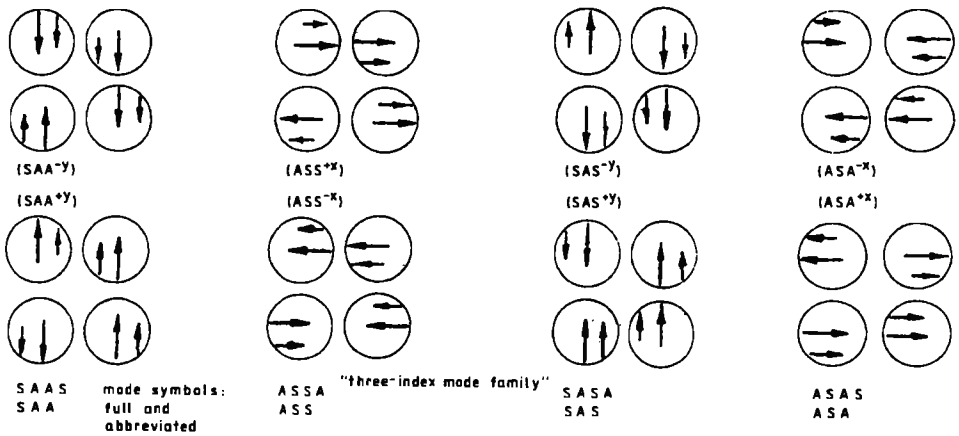

Fig. 15. Schematic representation of the transversal H field distribution of the fundamental SA modes in a single-mode quadruple-core optical fiber with square distribution of cores (called further fundamental SA modes). Field deformations against original HE_{11} mode distribution are overestimated here, to emphasize the influence of neighbouring cores and display effects of optical power coupling. This coupling influence results in the shifts of the fields in the cores against fiber axis, respectively inward and outward, but fully symmetrical. Three index SA modes family exhibits slight nonsymmetries in field distributions. Not all modal spots are equally spaced from fiber axis for this family. The inset with Cartesian coordinates is a key for the designation of mode symmetricity and abbreviated mode names, using "+" and "−" signs. Upper part of figure (p. 36) shows SA modes for twin-core optical fiber for comparison.

adjacent third core for $z = 0.125$. Then, nearly all power is coupled to the first core $z = 0.25$. The cores adjacent to the excited one are coupled equally but with the shift in fiber length.

Figures 16**c** and **d** show the calculated coupling curves for the same fiber, when two cores are excited. Core 4 in Fig. 16**c** maintains optical power for longer length than in other cases, while in the last case, presented in Fig. 16**d**, the coupling gets more homogeneous, in terms of optical power distribution among the cores.

Figure 17 shows one of the particular cases of signal power coupling in the quadruple-core optical fiber with square distribution of cores. Only one core is excited. Nearly the whole optical power goes periodically to the more distant core across the square (diagonal core), with both remaining cores acting again as symmetrical optical power relays. With two adjacent cores excited this core system is equivalent to twin-core geometry. With two diagonal cores excited the system is perfectly symmetrical and sums up and divides power equally between two remaining cores. The fiber inset with data shows the specimen of the same data as in previous cases of quadruple-core optical fibers.

Figure 18 shows a chosen coupling situation for quadruple-core optical fiber with homogeneous triangular distribution of cores. If the middle core is excited the picture is fully symmetrical and optical power in remaining cores is equal. The operation is a division by three (Fig. 18**a**). When one of the extreme cores is excited

T a b l e. Noncoupled and coupled fundamental modes in a single-mode quadruple-core optical fiber with square distribution cores (key to field values: o – field maximum, × – field minimum, : – field values reaches zero. Field symmetricity is considered against xy axes with Cartesian zero in the fiber ceter). Abbreviated mode symbol with a dash means coupled modes

No.	Mode name (fundamental group)	Mode symbol	Abbreviated mode symbol	Number of modes	Schematic field distribution	Comments
1.	Symmetric	SSSS	S	1	oo ×× oo ××	Basic field distributions with all cores excited
2.	Symmetric – antisymmetric	SSAA	SA	1	o× ×o o× ×o	
3.	Antisymmetric – symmetric	AASS	AS	1	oo ×× ×× oo	
4.	Antisymmetric	AAAA	A	1	o× ×o ×o o×	
5.	Symmetric SA	SASA	SAS	4	o× ×o oo ××	
	Symmetric AS	ASSA	ASS		×o o× oo ××	
	Antisymmetric AS	ASAS	ASA		oo ×× ×o o×	
	Antisymmetric SA	SAAS	SAA		oo ×× o× ×o	
6.	Coupled symmetric SA	S+SA	$\overline{SSA}$	12	o: ×: :o :× o: ×: :o :×	Coupled twin-core modes
	Coupled antisymmetric AS	A+AS	$\overline{AAS}$		SAS+SAA, ASA+ASS :o o: :× ×:	
	Coupled symmetric AS	S+AS	$\overline{SAS}$		:: oo oo :	
	Coupled antisymmetric SA	A+SA	$\overline{ASA}$		SAS+ASS, ASA+SAA o× :: :: o×	
	Coupled symmetric – antisymmetric	S+A	$\overline{SA}$		:o o: o: :o	
	Coupled antisymmetric – symmetric SA	SA+AS	$\overline{ASSA}$ or $\overline{SAAS}$		SAA+ASS, ASA+SAS o: :o :× ×:	

7.	Coupled symmetric SAS	S+SASA	$\overline{SSAS}$	8	:o : × o: × : :: :: oo × ×	Coupled single-core and three-core modes: anticlockwise commutation of mode pattern
	Coupled symmetric ASS	S+ASSA	$\overline{SASS}$		o: :o :: oo	
	Coupled symmetric ASA	S+ASAS	$\overline{SASA}$		:: oo o: :o	
	Coupled symmetric SAA	S+SAAS	$\overline{SSAA}$		:: oo :o o:	
	Coupled antisymmetric SAS	A+SAS	$\overline{ASAS}$	4	:: o × o: : o	
	Coupled antisymmetric ASS	A+ASS	$\overline{AASS}$		:: × o :o o:	
	Coupled antisymmetric ASA	A+ASA	$\overline{AASA}$		:o o: :: × o	
	Coupled antisymmetric SAA	A+SAA	$\overline{ASAA}$		o: :o :: o ×	
	Coupled symmetric-antisym. SAS	SA+SAS		8	:: o × :o o:	Clockwise coupled single-core mode pattern commutation
	Coupled symmetric-antisym. ASS	SA+ASS			:: × o o: : o	
	Coupled symmetric-antisym. ASA	SA+ASA			o: :o :: × o	
	Coupled symmetric-antisym. SAA	SA+SAA			:o o: :: o ×	
	Coupled antisymmetric-symmetric SAS	AS+SAS		4	o: :× :: oo	
	Coupled antisymmetric-symmetric ASS	AS+ASS			:o ×: :: oo	
	Coupled antisymmetric-symmetric ASA	AS+ASA			:: oo :o ×:	
	Coupled antisymmetric-symmetric SAA	AS+SAA			:: :: oo ×× o: ×: :× : o	

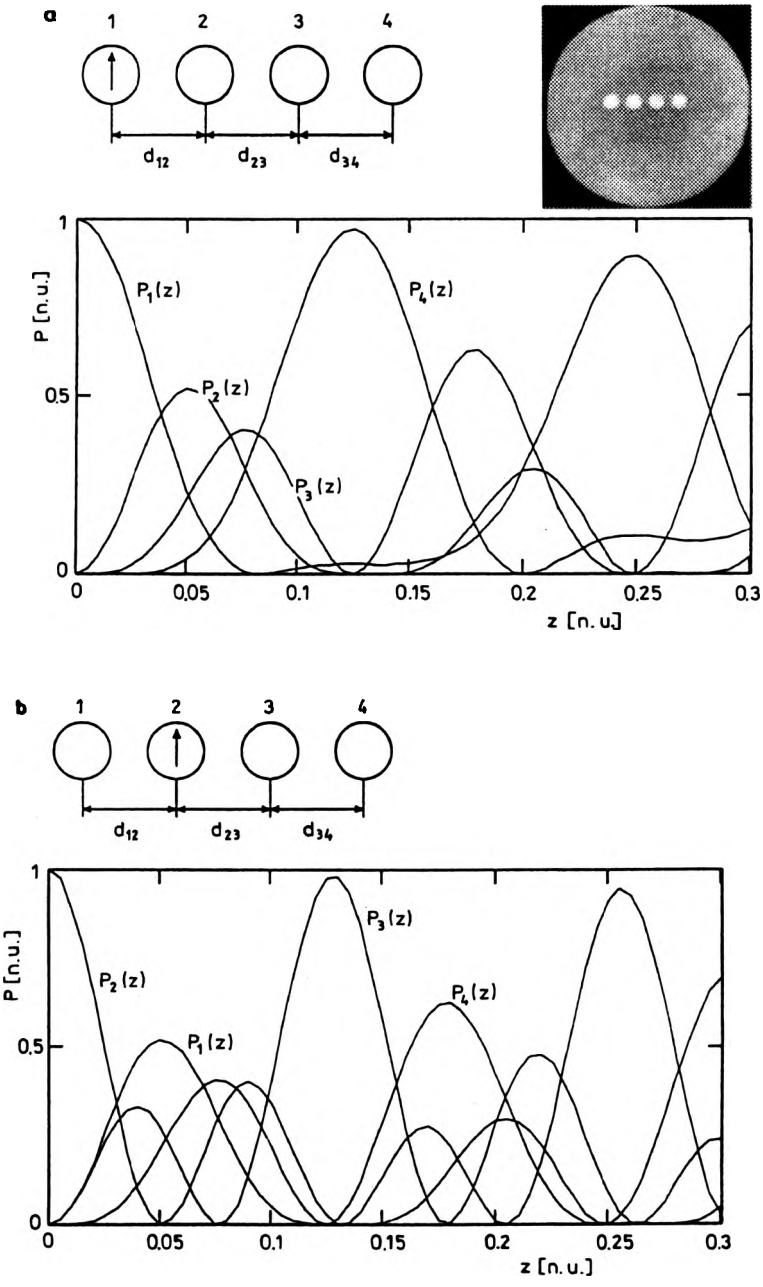

Fig. 16. Power coupling processes in quadruple-core optical fiber with linear distribution of cores. a — calculated power curves in individual cores with the extreme core excited. Back-coupling process to the excited core is "delayed". Virtually no optical power propagates in the excited core for comparatively broad range of normalized distances between $z = 0.075$ and $z = 0.175$. In this range the opposite extreme core receives and gives out nearly all the power. The inset with fiber single-mode quadruple core optical fiber with linear core distribution for which the calculations were performed. Fiber data is the same as in the previous cases: $\varnothing = 65$ μm, $2a = 4.8$ μm, $d = 7.5$ μm glass, set A. (to be continued on page 41)

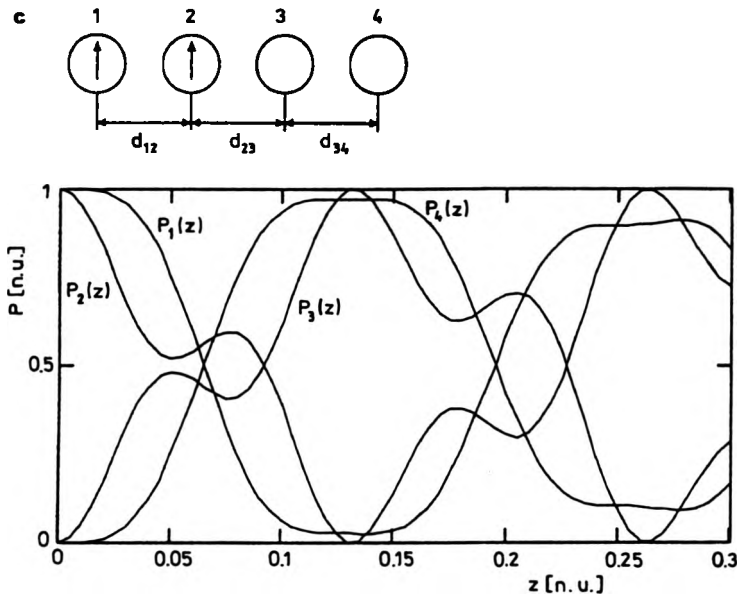

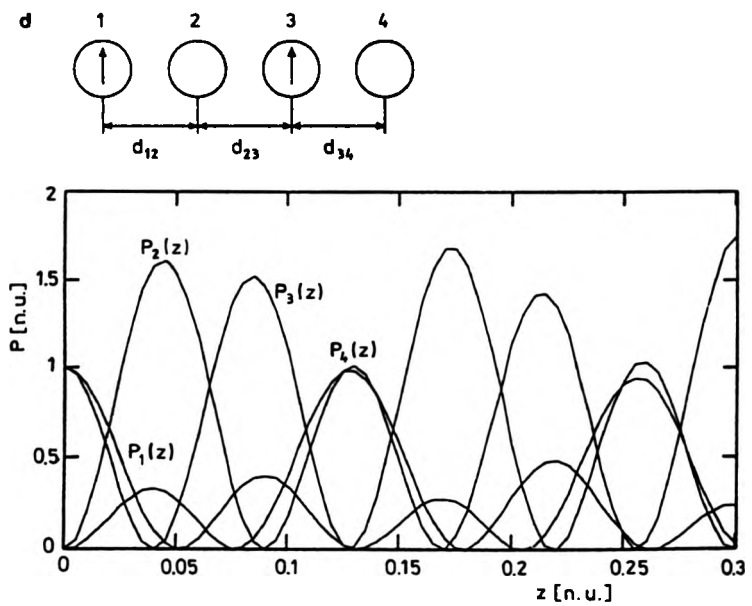

Fig. 16. (continued) This fiber is also a subject of further measurements. **b** — calculated coupled optical power curves for one of the inside cores excited. It is seen that the coupling from excited core is not equal to its both sides, resulting in nonsymmetrical coupling characteristics. **c** — Calculated coupled power characteristics for the same case with two adjacent cores excited including the extreme one. **d** — calculated coupled power characteristics with two non-adjacent cores excited simulatne- (continued on page 42)

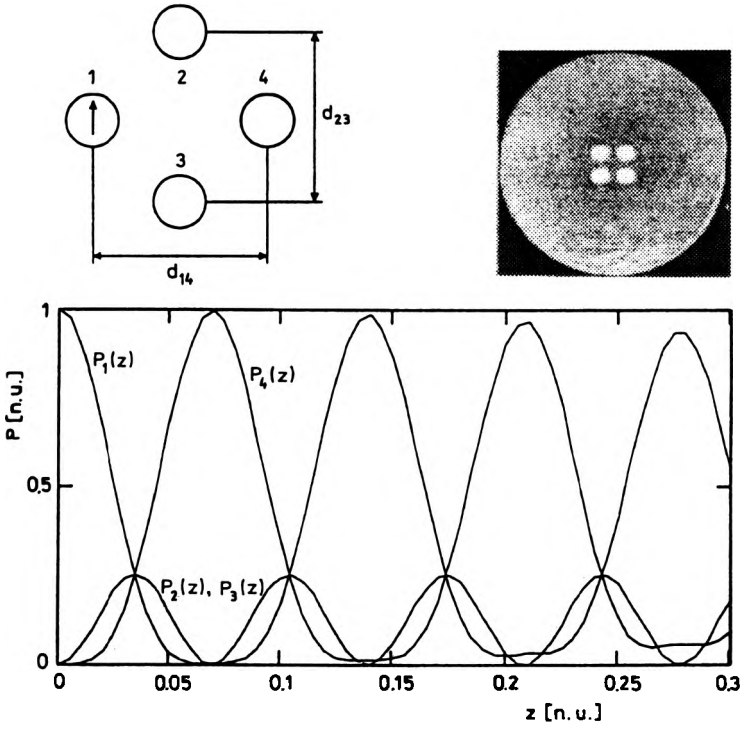

Fig. 17. Calculated coupling of optical power in a quadruple-core single-mode optical fiber with square distribution of cores. The optical power approach to coupling is alternative to field analysis approach. In the field approach we assumed, however, the simultaneous excitation of all cores, and coupling as the interference of fields. Optical power approach is an integral one through the Poynting vector analysis. One core (the first one) is excited in this case and the power summs up in the fourth one through symmetrically placed cores two and three. The inset with optical fiber photograph shows manufactured exemplary specimen for which the calculations were performed and which is subject of further measurements. Fiber data are similar to the previous cases: $\varnothing = 65$ μm, $2a = 4.8$ μm, $d = 7.5$ μm glass set A. The fiber can be covered with one more additional glass cladding to make its external diameter compatible with telecommunications standard of 120 μm, with no quoted parameters changed.

(Fig. 18**b**), the situation is a superposition of those presented in Figs. 3**a**, **c**. The fiber inset shows again a quadruple-core optical fiber of the same parameters as previously but triangular core distribution for comparison, checking the efficiency and flexibility of technology and further measurements of fiber properties.

Summing up, the major properties of single-mode quadruple-core optical fibers one can notice (Table and Fig. 15) unique feature of core commutation (clockwise

---

Fig. 16 (continued) ously. Optical power in the third core fades quicker than in the extreme core due to direct coupling of this core to cores two and four. The first core is coupled directly only to the second one and through it to the rest of cores, thus the coupling processes are shifted in phase in comparison with core three.

and anticlockwise) in this kind of fiber with square distribution of cores. This commutation can be explained solely on the basis of coupled fields analysis through the model of coupled SA modes. Another problem is practical fiber excitation in such a way as to obtain this effect. By commutation (a term taken from telecommunication technique) we understand coupled mode propagation in a fiber in the way that only one core carries optical signal at a time and the transmitting cores are switched periodically.

The next important feature of quadruple-core optical fiber is the possibility of resonant core coupling by technological choice of fiber parameters. The power curves can be shifted in phase against z axis in such a way as to be perfectly in phase with other power curves of adjacent cores [18]. This leads to strong wavelength selectivity of four-core optical fibers. One of the selectivity curves thus calculated for presented single-mode quadruple-core optical fiber with square distribution of cores is depicted in Fig. 19.

8. Photonic signal transmission and processing in multicore optical fibers

Multicore optical fibers are expected to give some new possibilities in signal transmission and processing. However, only few of these possibilities have been confirmed practically so far [18]. These possibilities stem from the unique physical

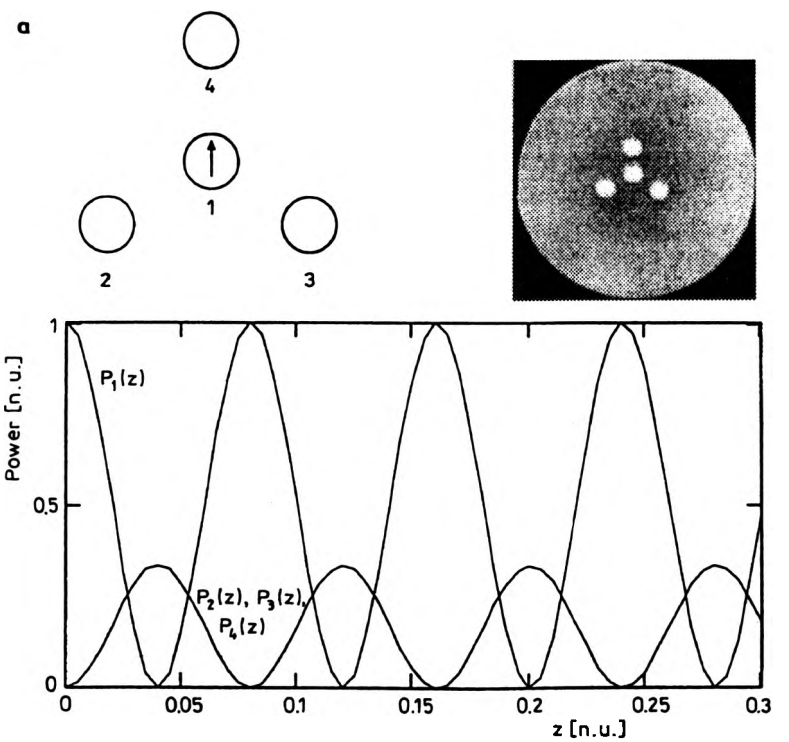

Fig. 18a

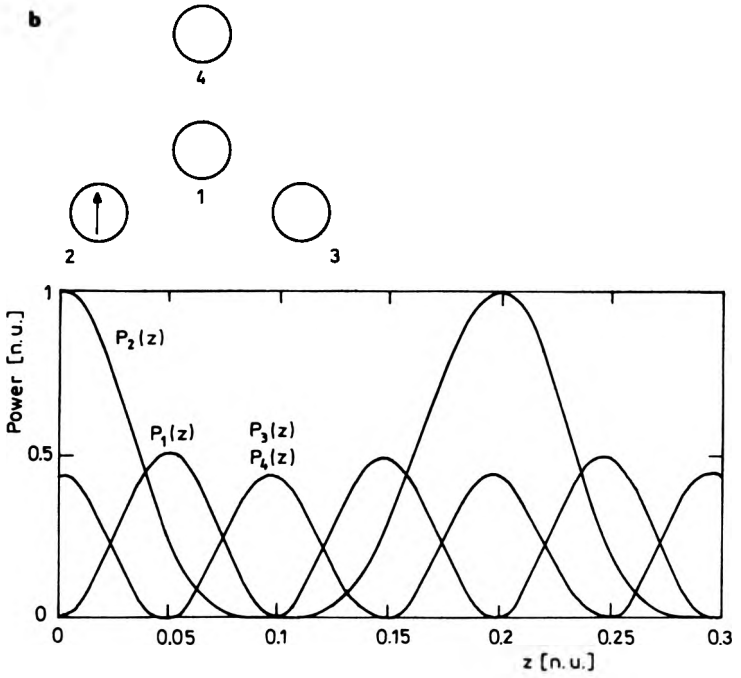

Fig. 18b

Fig. 18. Optical power coupling characteristics of quadruple-core single-mode optical fibers with triangular (equilateral – isosceles) distribution of cores. Fiber data (standardized fiber assumed for calculations and measurements through this work shown in the insert photograph) are nearly the same as in previous cases: $\varnothing = 65$ μm, $2a = 4.8$ μm, $d = 8$ μm, glass set A. **a** – middle core excited, power in circumferential cores nearly the same. **b** – one of circumferential cores excited. We assume in all optical power coupling analyses the losslessness of all coupling processes and losslessness of the fibers under analysis. This is nearly the truth as the fiber lengths for measurements are negligible for optical loss considerations.

structure of these fibers and resulting modal properties, which have been partly presented above. Perhaps, the three most important features out of these are:

- wave interference between cores [14],
- signal multiplexing between cores [11], and
- multi-channel transmission [1].

All of the features may be used for different purposes. For example, the multi-channel feature of MOF may be used for an increase of the bit error rate (BER), transmission stabilization and increase of reliability.

The feature of inter-core wave interference gives the photonic system designer a tool for potential making of an intrinsic interferometer inside a single optical fiber. Two or more cores in a MOF may serve simultaneously as signal and/or reference channels. Intrinsic MOF interference is inseparably combined with single-mode wave transmission in strictly parallel, closely spaced, and neighbouring cores in a single fiber cladding. A bigger number of cores than two, depending on their mutual coupling, may be used for realization of a more complex structure of the

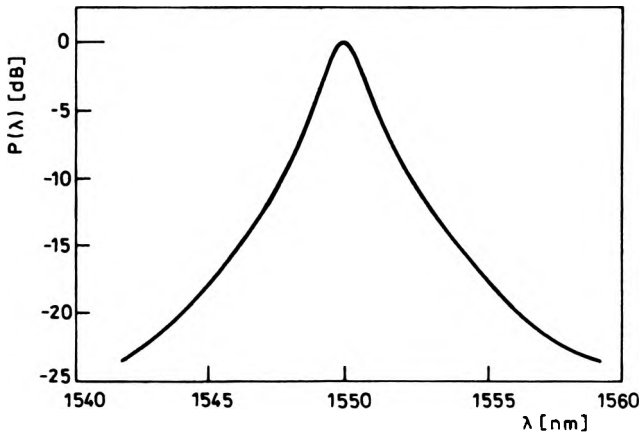

Fig. 19. Calculated optical output power wavelength selectivity curve for investigated quadruple-core single-mode optical fiber. The output power is from core number four from Fig. 17, when core number one is excited.

interferometer (like quadruple interferometry, wave quadrature detection, *etc.*) or increasing system parameters such as signal to noise ratio (SNR), and decreasing BER. This also potentially allows the introduction of doubled reference channels, forward and reverse hand-shaking channels, introduction of constant delay in signal transmission or constant difference in optical signals pathways, and many more.

The comparison of a single MOF fiber interferometer with a more classical geometry with at least two fibers, for example, in Mach–Zehnder or other classical topologies, reveals the substantial differences between both solutions. In different potential applications, some of these features may be advantageous and some disadvantageous. The interferometer with single fibers has separate signal channels in both legs. The legs are distributed in the measuring space arbitrarily. The reference leg can be tuned arbitrarily. Not all of these features concern a MOF based fiber interferemeter. The properties of the sensing interferometric loop, or its sensitivity are achieved technologically by changing the MOF parameters, such as distance between individual cores, which is the most basic parameter determining the core coupling, numerical apertures of individual cores (also influencing considerably the core coupling), core diameters, refractive index profiles of individual cores, absolute values of refractive indices in the cores, cladding and in the area between adjacent cores.

The change of absolute sensitivity in a classical interferometer requires changing the optical path-length in the measuring leg of the device. The change of absolute sensitivity of a single MOF based interferometer requires that nearly all technological parameters of the fiber be changed. A single MOF based interferometer has usually, according to our experiences, somehow smaller sensitivity in comparison with similar classical fiber-optic interferometers. One can realize,

however, a multiple MOF based interferometer, which changes substantially the picture. A multiple MOF based interferometer design adds a few very interesting features to the classical solution.

The possibility of multiplexing optical signal among the particular cores in a MOF is connected with the presence of a few potentially coupled cores. The coupling process can have intrinsic nature, as well as can be forced by external influence on the MOF fiber. The coupling process can thus be intrinsic, extrinsic, passive or active, natural or forced. This intrinsic property of the MOF is a novel valuable tool for design of the following systems and devices:

– transmission channels with core division multiplexing (CDM, analogously to WDM, TDM, *etc.*),

– photonic functional devices like: couplers, switches, keys, optical insulators, non-reciprocal transmissive components, filters, *etc.*,

– MOF based photonic sensors, which may use CDM, MOF intrinsic interference (MOFII) and multi-channel transmission (MOFMT).

In particular, the signal switching or multiplexing (either passive or active) may be used for construction of a MOF based movement transducer. The optical signal is switched between non-coupled cores. The switching is performed at the end face of the fiber in the free space. This kind of multicore reflective device may be used for tactile sensing, touch sensing, shape definition sensing, object presence sensing, object movement, *etc.*

The wave switching can be performed inside a MOF along the fiber at particular points or in a more distributed way along the whole (or not whole) length of the transmission channel. This may lead to either distributed multi-point sensing or distributed photonic signal processing. Such MOF based components have a potential to enhance the construction and theory of distributed multi-node all-photonic networks.

The third feature, separate multichannel transmission ability, is a base for introducing some controlled redundancy to the system based on MOF. Transmission of the same signal in the MOF cores is sometimes an unnecessary redundancy. Perhaps, it is justified in the case of weak transmission with accidental signal fading or harmful interference. Cumulative signal detection from separate cores is possible in these cases. The separate core signals can be treated as correlated, which as regards the photonic receiver enhances the transmission system performance. The separate core transmission channels can be used for hand-shaking, reverse acknowledgement, protocol checking, operator alarms and service, system maintenance and power-on-self-tests procedures, transient, dynamic, photonic information buffering, *etc.*

The MOF transmission redundancy can be used for:

– Stabilization and linearization of photonic transmitters and/or receivers. The photonic signal is sent back proportionally to the level of received power at the receiver, which in turn tunes the transmitter. This way serves system optimization,

power consumption minimization, SNR optimization, system reliability improvement, signal quality enhancement, *etc.*

– Creation of photonic network pulse loop devices, with the signal looped in a single MOF fiber, for signal processing (in-flight memory, delayed multi-channel detection, *etc.*).

– Realization of transmission channels with multi-factor flow for cryptography, multiple signal checking of bit-after-bit type, multilevel transmission signals coding, novel coding methods, *etc.*

– Realization of all-photonic (transparent) information buses. The MOFs can be used there for: transmission lines, photonic signal guided wave processing channels, coherent detection components, interferometric legs, functional components, such as couplers, insulators, power switches, components in electrooptical subsystems, *etc.*

There are also different methods of signal processing in the MOF. They are connected with the geometrical structure of these fibers, properties of complex, individual gradient refractive index profiles, specially designed core material properties, shapes of the cores, coupling between cores and the outer world (closeness of cores to the outer cladding boundary), presence of refractive traps in the fiber, *etc.* The MOF allows potentially the selective signal division, signal separation, signal summing and subtracting, realizing optical insulation, unidirectionality, *etc.* Potentially, the MOF components embrace: simple and complex couplers, tapered and non-tapered devices, mode converters, wavelength filters, bent filters with different sensitivities to the fiber bending from different cores, selective attenuators, *etc.*

The hetero-core MOFs allow potentially the selective waves attenuation in chosen channels. The signal which is to be attenuated, in a MOF active photonic channel, is switched, at preset place along the path, to a special core of high losses. The signal, after reaching desired level, is switched back to the transmissive low-loss channel. In reverse the hetero-core MOFs allow potentially the selective signal amplification. The signal which is to be amplified in a MOF active photonic channel is switched, at preset place, to a special amplifying core (rare earth doped core amplifier). The signal after reaching desired level is switched back to the transmissive low-loss channel.

Mode conversion, signal coding, timing, code re-grouping, pulse sequence separation, totally photonic multiplexing and demultiplexing may be potentially done totally inside a single hetero-core (different core dimensions, numerical apertures, refractive profiles, absolute refraction, material properties) MOF using either intrinsic or extrinsic (and natural or forced) transmission phenomena. Single-mode cores in a MOF of properly chosen cut-off wavelength and coupled with a defined main photonic power transmission channel may potentially couple off efficiently a chosen waveguide mode from this channel. On the other hand, a few single-mode transmission channels may couple their signals on a common multi-

mode channel. There are a lot of ideas of this kind. Some of them, or perhaps quite different with the use of MOFs, may turn practical in the near future [18], [19].

9. Conclusions

It is for the first time that there have been presented and compared in a single work some common properties of a few simplest families of single-mode multicore optical fibers including twin, double, triple and quadruple ones with homogeneous distribution of cores in the cladding. Coupled modal fields and optical power analysis was performed to gain an insight into core coupling. The understanding of coupling processes in single mode multicore optical fibers is needed to optimize the technology of such unique filaments at the FOD of Biaglass Co.

This work gathers a bunch of useful dependences allowing calculation of some basic parameters of multicore optical fibers. A number of samples of triple-, double-, twin- and quadruple-core optical fibers were manufactured, modelled and measured using the theory quoted. Due to their unique modal properties, the MOFs awake expectations for numerous research applications in photonic systems.

A number of specific individual properties of some MOFs have been predicted theoretically and in some cases confirmed by measurements [20], and these include:

– Some models of double-core and twin-core optical fibers were investigated theoretically for the purpose of technological optimization during the pulling processes of these fibers. Effective power transfer efficiency in some examples of double-core optical fibers was shown to be a function of a very narrow-band wavelength (Fig. 5). Very efficient optimization of propagation and signal processing properties of this family of fiber was shown to be possible (Fig. 7). Beating lengths in manufactured specimens of these fibers were calculated and measured for some samples.

– Resonant coupling phenomenon was predicted in three-core optical fibers (Fig. 3a). A complete power transfer is predicted to be possible only under these coupling conditions, otherwise the coupling seems to be partial (Fig. 3c). We have calculated and measured for one example the beating length for three-core optical fibers (Figs. 9 and 10).

– It was shown for the first time [14] that the model of SA modes describes very well the phenomena of core coupling in the family of quadruple-core single-mode optical fiber with square distribution of cores. This was partially confirmed by analysing some of these same fibers with integrated power flow method. Efficient selective power coupling was observed among the cores. Resonant coupling was also predicted in these fibers to result in wavelength selectivity of some of these fibers (mostly with different core parameters). Some of the coupling characteristics of four-core optical fibers were shown to have characteristics competitive in selectivity to other WDM devices (Fig. 19).

References

[1] ROMANIUK R., DOROSZ J., *Coupled/noncoupled wave transmission in long-length of multicore optical fibers*, Proc. 10th European Conf. on Optical Communication, Stuttgart, Sept. 3–6, 1984, VDE Verlag, pp. 202–204.
[2] SNYDER A. W., LOVE D. J., *Optical Waveguide Theory*, Chapman and Hall, New York 1984.
[3] WIJNGAARD W., J. Opt. Soc. Am. **63** (1973), 944.
[4] JABŁOŃSKI T., SOWIŃSKI M., Proc. SPIE **670** (1986), 30.
[5] ROMANIUK R. S., POŹNIAK K. T., *Photonic telemetric network*, Technical Report, Institute of Electronic Systems, Warsaw University of Technology, Priority Program: *Photonics engineering*, Warsaw, December 1998, 70 pages.
[6] KITAYAMA K., ISHIDA Y., J. Opt. Soc. Am. A **2** (1985), 90.
[7] SALATHE R. P., GILGEN H., BODMER G., Opt. Lett. **21** (1996), 1006.
[8] KISHI N., YAMASHITA E., ATSUKI K., J. Lightwave Technol. **4** (1986), 991.
[9] KISHI N., YAMASHITA E., KAWABATA H., J. Lightwave Technol. (1989), 902.
[10] TJUGARTO T., CHU P. L., PENG G. D., Opt. Lett. **17** (1992), 1058.
[11] ROMANIUK R., DOROSZ J., Telecommunication Review **60** (1985), 9 (in Polish).
[12] ROMANIUK R., DOROSZ J., Proc. SPIE **722** (1986), 117.
[13] ZDRODOWSKI K., *Analysis of light propagation in multi-core optical fibers*, M.Sc. Thesis, Technical University of Białystok, 1997.
[14] ROMANIUK R., Proc. SPIE **1085** (1989), 214.
[15] DOROSZ J., *Crucible technology of multicore optical fibers*, Research Dissertations of Technical University of Białystok, Vol. 29, Białystok 1995 (in Polish, contains English summary).
[16] DOROSZ J., *Theoretical and practical problems of multicore fiber optic technology*, Research Dissertations of Technical University of Białystok, Vol. 41, Białystok 1997 (in Polish, contains English summary).
[17] ROMANIUK R., DOROSZ J., *Modification of MMC technology for twin and double core optical fibers*, Technical Report, Warsaw University of Technology, January 1999, Priority Program of WUT: *Photonic engineering* (in Polish).
[18] DOROSZ J., ROMANIUK R., Proc. SPIE **3577** (1998), 9.
[19] ROMANIUK R., DOROSZ J., Proc. SPIE **3577** (1998), IV.
[20] DOROSZ J., ROMANIUK R., *Multicore optical fibers*, Internal Technical Report, Biaglass Co., December 1998 (in Polish).

Received October 19, 1998
in revised form February 15, 1999